EHL ANALYSIS WITH ACTUAL REE-EYRING MODEL

A DISSERTATION SUBMITTED

IN THE FULFILMENT OF THE REQUIREMENT FOR THE AWARD OF THE DEGREE OF

MASTER OF TECHNOLOGY

IN

MECHANICAL ENGINEERING

(MACHINE DESIGN)

BY

LALIT VASHISHTH

208440

UNDER THE GUIDANCE OF

DR. S. S. RATTAN

DR. PUNEET KUMAR

DEPARTMENT OF MECHANICAL ENGINEERING

NATIONAL INSTITUTE OF TECHNOLOGY

(Institution of National Importance)

KURUKSHETRA – 136119

2008-2010

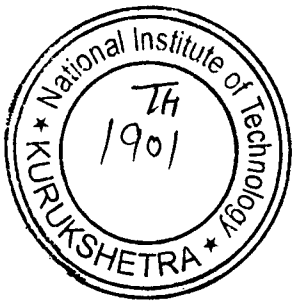

CERTIFICATE

This is to certify that **Mr. Lalit Vashishth**, Roll no. **208440** has successfully completed his dissertation entitled "**EHL Analysis with Actual Ree-Eyring Model**" being submitted in the partial fulfillment of the requirements of the award of degree of **Master of Technology** in **Mechanical Engineering (Machine Design)** at **National Institute of Technology, Kurukshetra** is an authentic record of original work carried out by him under our guidance and supervision.

The work embodied in this dissertation is his bonafide research work, and has not been submitted elsewhere for the award of any other degree or diploma.

(Dr. S.S. Rattan)
Professor
Mechanical Engg. Deptt.
National Institute of Technology
Kurukshetra-136119, India

(Dr. Puneet Kumar)
Assistant Professor
Mechanical Engg. Deptt.
National Institute of Technology
Kurukshetra-136119, India

ACKNOWLEDGEMENT

This project has been possible by the bountiful mercy and grace of God. It is my great pleasure to express my thanks to all the magnanimous persons who rendered their full support to my work directly or indirectly.

First and foremost, I would like to express my thanks and indebtedness to my guide Dr. S.S. Rattan, Professor (H.O.D.), and Dr. Puneet Kumar, Associate professor, Mechanical Engineering Department, National Institute of Technology, Kurukshetra, for their deep involvement, invaluable and continuous motivation throughout this work.

Finally, I would like to dedicate this project work to my parents & my friends who are great source of support & encouragement, especially in all of our academic endeavors.
Very special thanks dedicated to Dr. Puneet Kumar.

Lalit
(LALIT VASHISHTH)

ABSTRACT

Lubrication involves the separation of the surfaces pressed against each other under load and in relative motion by introducing a layer of fluid between them. In the case of hydrodynamic lubrication a fluid film is produced between the contacting surfaces and the pressure generated in the film balances the applied load. A special form of hydrodynamic lubrication, elastohydrodynamic lubrication (EHL), is genrally encountered in mechanical components involving highly stressed non-conformal contacts such as gears, cams, roller bearings etc. EHL is characterized with substantial elastic deformation of the interacting surfaces and piezo-viscous rise in lubricant viscosity which assist largely in the evolution of the load carrying fluid film.

In the present work, the shear thinning behaviour of three oils namely LF 5346, PG 460 and PDMS in EHL line contacts is studied using actual Ree-Eyring model. The modified Reynolds equation incorporating the effect of non-Newtonian fluid is derived using perturbation method and the governing equations are discretized using finite difference scheme. The discretized Reynolds equation is solved iteratively along with the load balance condition using the robust Newton-Raphson scheme. A computer code is developed for the implementation of the solution algorithm.

A comparison between the well established Carreau model and Ree-Eyring model is shown for the aforesaid oils. The departure from Carreau model can be minimized by increasing the number of flow units. Also, it has been shown that the most widely used sinh law either underestimates or overestimates the shear-thinning effect to a great extent.

In this dissertation, the effect of various operating parameters such as load, slide to roll ratio, speed and radius on minimum film thickness, central film thickness and coefficient of friction etc is studied. It has been shown that the actual Ree-Eyring model can capture the effect of increased load and scale sensitivities of EHL film thickness pertaining to shear-thinning fluids.

List of figures and tables

NOMENCLATURE

DIMENSIONAL PARAMETERS

b : half width of Hertzian contact zone, (m)

E : effective elastic modulus of rollers 1 and 2 (Pa)

h : film thickness (m)

h_{min} : minimum film thickness (m)

h_0 : offset film thickness (m)

p : Pressure (Pa)

p_h : maximum Hertzian pressure, $p_h = E'b/4R, (Pa)$

R : equivalent radius of contact (m).

u : local fluid velocity (m/s)

u_0 : average rolling speed, $u_o = (u_o + u_b)/2, (m/s)$

u_a, u_b : velocities of lower and upper surfaces, respectively (m/s)

v : surface displacement (m)

w : applied load per unit length (N/m)

x : abscissa along rolling direction (m)

x_i : flow unit

y : ordinate across the fluid film (m)

Greek symbols:

α : piezo-viscous coefficient (Pa^{-1})

γ : shear strain rate across the fluid film, $\gamma = \frac{du}{dy}, \left(s^{-1}\right)$

ρ_0 : inlet density of the lubricant (kg/m^3)

ρ : lubricant density at the local pressure (kg/m3)

τ : shear stress in fluid (Pa)

η_0 : inlet viscosity of the Newtonian fluid (Pa–s)

η : Fluid viscosity (Pa–s)

NON-DIMENSIONAL PARAMETERS

f_1 : residue of discretized Reynolds equation at *i*-th node

G : non-dimensional material parameter, $G = \alpha E'$

H : non-dimensional film thickness, $H = hR/b^2$

H_{min} : non-dimensional minimum film thickness, $H_{\min} = h_{\min} R/b^2$

H_0 : non-dimensional offset film thickness, $H_0 = h_0 R/b^2$

K : lumped constant in Reynolds equation, $K = 3U\pi^2/\left(4W^2\right)$

N : total number of nodes

P : non-dimensional pressure, $P = p/p_h$

S : slide to roll ratio, $S = (u_b - u_a)/u_0$

$\bar{u}$: normalized local velocity of fluid, $\bar{u} = u/u_0$

U : non-dimensional speed parameters, $U = \frac{\eta_o u_o}{ER}$

$\bar{v}$: non-dimensional displacement, $\bar{v} = vR/b^2$

W : non-dimensional load parameter, $W = \frac{w}{E'R}$

X : non-dimensional abscissa, $X = x/b$

X_m : inlet boundary co-ordinate

X_{max} : maximum value of X = x/b used in the mesh

X_N : X-co-ordinate at N-th node

X_0 : outlet boundary co-ordinate

ΔX : grid size of mesh

Y : non- dimensional y coordinate, $Y = y/h$

z_0 : Roelands parameter.

Greek symbols:

$\bar{\rho}$: non-dimensional fluid density, $\bar{\rho} = \rho/p_0$

$\bar{\tau}$: non-dimensional shear stress, $\bar{\tau} = \tau / E'$

$\hat{\tau}$: shear stress normalized by limiting shear strength, $\hat{\tau} = \tau / \tau_L$

$\bar{\eta}$: non-dimensional viscosity of Newtonian fluid, $\bar{\eta} = \eta / \eta_o$

MATRICES AND VECTORS

[F] : residual vector in Newton-Raphson formulation

[J] : Jacobian matrix in Newton-Raphson formulation

[Δ] : vector of corrections in system variables

ABBREVIATIONS

EHL : elastohydrodynamic lubrication

CONTENT Page No.

Chapter 1

INTRODUCTION

Lubrication is essential for the separation of surfaces in relative motion and pressed together under load for the minimization of fiction and wear. In the case of hydrodynamic lubrication, a fluid film is produced between the contacting surfaces and the pressure generated in the film balances the applied load. The study of the hydrodynamic lubrication by taking into account the elastic deformation of contacting surfaces and piezo-viscous increase in lubricant viscosity is known as elastohydrodynamic lubrication (EHL). In other words, Elastohydrodynamic lubrication [1] can be defined as a mode of hydrodynamic lubrication where the elastic deformation of the contacting bodies and the increase in viscosity with pressure play a fundamental role in the evolution of a sufficiently thick load carrying fluid film. The influence of elasticity is not restricted to secondary changes in load capacity or friction as in the case of hydrodynamically lubricated pivoted pad and journal bearings. Instead, the elastic deformation of the interacting surfaces has to be included in the basic model of elastohydrodynamic lubrication. The same is true for piezo-viscous increase in viscosity.

The existence of EHL films was speculated long before it could be established using specific physical concepts. The lubrication mechanism in conformal contacts such as those encountered in hydrodynamic and hydrostatic bearings were well defined and the reasons for their effectiveness were well understood. However, the mechanism of lubrication pertaining to highly stressed non-conformal contacts in mechanical components such as gears, rolling contact bearings, cams and tappets etc remained unexplored. The wear rates of these components were very low which indicated the existence of films sufficiently thick to separate the surfaces. However, this conclusion was not in agreement with the calculated values of hydrodynamic film thickness for the operating conditions typical of the aforesaid components. The predicted values of film thickness were so low that it was impossible for the contacting surfaces to be separated

by a viscous liquid film. In fact, the calculated film thickness suggested that the surfaces were lubricated by monomolecular films. However, much higher wear rates and friction coefficients were obtained when experiments involving such ultra-thin lubricant films were carried out. This apparent contradiction between the empirical observation of effective lubrication and the limits of known lubrication mechanisms could not be explained for a considerable period of time. In order to bridge this gap, a host of researchers made countless attempts which culminated in the evolution of EHL theory.

The successful operation of mechanical components operating in EHL depends upon the existence of a fluid film as thin as a few hundred nanometres or even thinner. Therefore, it is important to be able to predict the fluid film thickness and traction coefficient under a given set of operating conditions at the design stage. Therefore, several efforts have been made over the last five decades in order to study the EHL behaviour for a wide range of operating conditions. The early theoretical investigations relied upon simplified analyses employing Newtonian fluid model which failed to explain the realistic film generation and traction behaviour. Therefore, the focus of attention shifted to more realistic and complex situations.

One of the most important physical effects to be considered in EHL analysis is the shear-thinning behaviour of EHL lubricants such as synthetic oils and mineral oil/polymer blends. The constitutive (shear stress-shear strain rate) relationship – often referred as rheology – obeyed by such lubricants has been the subject of extensive research. A detailed review of the relevant literature is presented in Chapter 2 of this dissertation. Amongst the several rheological models proposed by the researchers, the inverse hyperbolic sine law – often attributed to Ree-Eyring has been the most widely used shear-thinning model. However, some recent studies have revealed that the so called Ree-Eyring model fails to describe the experimental flow behaviour as well as EHL film-thinning behaviour of lubricants. In fact, the actual Ree-Eyring model consists of multiple flow units in contrast to a single flow unit used in the popular (however,

incorrect) form of Ree-Eyring model. Therefore, the present work aims at investigating the various aspects associated with actual Ree-Eyring model using full EHL simulations. The modified Reynolds equation incorporating the effect of non-Newtonian fluid model is derived using perturbation method. This is described in Chapter 3 along with the numerical scheme used for solving the EHL model. Chapter 4 presents the detailed algorithm used in the solution procedure. The results presented and discussed in Chapter 5 include the comparison of various EHL characteristics like central film thickness, minimum film thickness, pressure distribution and coefficient of friction for different type of lubricating oils - LF5346 gear oil, PG 460 oil and PDMS oil. It is found that the number of flow units in actual Ree-Eyring model affect the degree of accuracy with respect to real shear- thinning behaviour. Finally, Chapter 6 includes the salient conclusions and the scope for future work.

Chapter 2

LITERATURE REVIEW

2.1 Historical Perspective of EHL

Dowson and Higginson [3] presented an account of the evolution of early EHL theory which is summarized in the following text. The study of contact conditions in gears revealed the possibility of fluid film lubrication in heavily loaded contacts. Operating experience showed that severe metal to metal contact was not taking place, and this led to the initiation of theoretical investigation of the lubrication problem. Martin [4] presented one of the earliest solutions to the lubrication problem by using an equivalent kinematic model of a cylinder near a rigid plane, with an incompressible and isoviscous lubricant. While being a good start, Martin's load formula could not predict effective lubricant film thickness.

The extension of the classical hydrodynamic theory to include the effect of elastic deformation was first carried out by Peppler [5] who determined the maximum oil film pressure which could occur between a pair of gear teeth lubricated by an isoviscous lubricant. It was concluded that the maximum oil film pressure could never exceed the corresponding maximum Hertzian contact pressure.

Meldahl [6] investigated the effect of high pressure on film shape and pressure distribution for a constant viscosity lubricant. The expressions for the surface displacements of a semi-infinite elastic solid subjected to an arbitrary loading were derived and by coupling these equations with Reynolds equation, a satisfactory solution to the problem was determined. However, due to poor convergence and cumbersome calculations involved, only one result could be produced.

The second extension to the lubrication theory was first considered by Gatcombe [7] when he investigated theoretically the effect of viscosity-pressure relationship on film

formation. Gatcombe [7] solved the Reynolds equation for a particular viscosity-pressure relationship assuming arbitrary boundary conditions. Although an increase in the lubricant film thickness was reported, it was not sufficient enough to allow formation of satisfactory lubricant film between gear teeth.

In an investigation of film thickness between teeth of rigid gears, started by Hersey and Lowdenslager [8], a parabolic viscosity-pressure relationship was assumed. Broadly, the change in the theoretical load carrying capacity from the isoviscous prediction was found to be in consonance with the improvement reported by Gatcombe for an exponential relationship. These developments attracted the attention of several investigators leading to a more rigorous analysis of the problem.

Dorr [9] re-investigated the problem of elastic contacts lubricated by an isoviscous fluid. He developed an iterative solution procedure in which the pressure distribution obtained in one stage was used to calculate the surface displacements, which were added to the initial shape of the contacting solids to produce a slightly different lubricant film shape. The new film profile was used to re-calculate the pressure distribution and the process was repeated until the convergence of film shape and pressure profile.

Earlier, Grubin [10] analysed the problem theoretically and produced an excellent account of the physical mechanism of the elastohydrodynamic lubrication. Although his solutions did not satisfy the elasticity and lubrication equations throughout the entire contact, the analysis of the inlet zone proved to be particularly useful. The film thickness values calculated were found to be greater than the corresponding predictions of Martin's theory by several orders of magnitude, which was consistent with the observation of satisfactory film formation in gear contacts. Besides the inlet zone analysis, Grubin also discussed the distribution of pressure in the contact region qualitatively. It was concluded that the pressure curve would exhibit a second maximum near the outlet end of the contact zone. Grubin's work represented the first successful examination of the combined effects of high pressure on the lubricant and the contacting surfaces.

The predictions of Grubin were confirmed by Petrusevich [11] when he obtained solutions for three different speeds which satisfied the governing elastic and hydrodynamic equations simultaneously. These solutions, which are now considered as general characteristics of the heavily loaded lubricated contacts.

Weber and Saalfeld [12] found out an interesting closed form solution to the elastohydrodynamic lubrication problem, which considered both constant and pressure dependent viscosity. The solution was, however, limited to small deformations and it could not distinguish between near Hertzian solutions which frequently occur in the practical situations.

The development of the theory of elastohydrodynamic lubrication required reliable quantitative experimental data pertaining to lubricating films in heavily loaded elastic contacts. In this regard, disc machines were built to simulate gear tooth contact and were used primarily to find the suitability of metals and lubricants for gear operating conditions.

A revolution in disc machine experiments was initiated by Crook [13] as the direct measurement of oil film thickness was reported by capacitance and oil flow methods. Crook found that at low loads the oil film thickness was inversely proportional to the load and directly proportional to speed as predicted by Martin's theory for rigid cylinders lubricated by an isoviscous fluid. At higher loads, which are representative of the operating conditions in gears, the film thickness in pure rolling was found to be almost independent of the load. This was in consonance with the predictions of Grubin's film thickness formula. Furthermore, the measured film thickness at high loads was found to be much higher than those predicted by Martin's theory and the typical value of 1 μm quoted by Crook was consistent with the idea that a continuous oil film may exist between gear teeth.

Crook [14] further extended the above investigations by considering the influence of speed and viscosity on film thickness. One of the major conclusions was that the viscosity of the lubricant at the surface temperature of the discs was of the greatest importance in the determination of the oil film thickness.

Subsequent investigations by Crook [15] revealed that rolling friction under elastohydrodynamic conditions is independent of the load and is proportional to the oil film thickness. The measurements of effective viscosity led Crook to suggest that the visco-elastic behaviour of the lubricant may be important.

An alternative experimental approach was described by Sibley and Orcutt [16] when presented film thickness measurements based upon X-ray transmission technique. The film thicknesses so measured, were in agreement with the Crook's measurements and the current elastohydrodynamic theory. Hence, all these experimental investigations supplied valuable data useful for the development of elastohydrodynamic lubrication theory.

Dowson and Higginson [17] presented a new approach to elastohydrodynamic theory. By introducing a solution of the inverse hydrodynamic lubrication problem, Dowson and Higginson were able to obtain satisfactory solution of the elastic hydrodynamic equations after a small number of cycles. The viscosity-pressure relationship for an actual lubricant was utilized in the analysis and the solution was obtained for a range of loads at a constant speed. Although most of the characteristics of the solution were consistent with Petrusevish's results, a noteworthy difference was the absence of the second high pressure peak.

The discrepancy was explained when Dowson and Higginson [18] reported further solutions which covered a wide range of loads, speeds and material properties. It was found that the existence and form of the second peak was a function of all these variables. In particular, the value of a dimensionless material parameter formed by the exponential viscosity-pressure coefficient for the lubricant and the effective elastic

modulus for the solids was shown to be influential in the determination of pressure distribution in a heavily loaded tact.

Dowson and Higginson [19] analysed their solutions and found that a convenient dimensionless formula for minimum film thickness could be written in terms of the load, speed and material parameters. The close agreement between the theoretical minimum film thickness predictions and the experimental results obtained by Crook and Sibley demonstrated that the gap between theory and experiments had been largely closed. In order to show the influence of speed and lubricant compressibility on a theoretical solution to the elastohydrodynamic lubrication a survey of isothermal solutions was presented by Dowson et al. [20]. Speed was shown to be the most important variable in the problem and the lubricant compressibility was found to have an appreciable influence on pressure distribution but little effect on minimum film thickness.

Sternlicht et al. [21] considered the distribution of pressure and temperature in highly loaded contacts. The introduction of an energy equation considerably increased the computational work required, but by employing finite difference method and a digital computer a successful iterative procedure was established.

The improved understanding of highly loaded lubricated contacts called for re-examination of the mechanism of fatigue failure. The well known type of failure is known as pitting was investigated and the role of lubricant clearly indicated by Dowson [22]. The Hertzian ellipse of dry contact was previously employed as the distribution of surface stress associated with highly loaded contacts. But the elastohydrodynamic theory showed that this distribution of pressure may be considerably modified in the presence of a lubricant.

Bell [23] contributed an interesting analysis of the effects of the non-Newtonian behaviour by considering the lubrication of rolling surfaces by sinh-law based rheological model which is popularly known as Ree-Eyring fluid. It was concluded that

at high rates of shear the effect of velocity on film thickness should diminish, whereas that of load should increase.

Milne [24], Tanner [25] and Burton [26] also studied the effect of non-Newtonian behaviour of the lubricant in rolling contacts. Once the existence of a coherent fluid film in some highly loaded contacts had been established, the coefficient of friction became the subject of several investigations.

Misharin [27] found that the coefficient of friction between two rollers obeyed the laws of elastohydrodynamic lubrication theory as developed by Petrusevich. He found that the friction coefficient increased as the operating temperature was raised and that it decreased slightly with an increase in either the sliding or rolling velocity.

2.2 Governing Equations

2.2.1 Reynolds equation

The equation which governs the generation of pressure in lubricating films is known as Reynolds equation and it forms the foundation of hydrodynamic lubrication analysis. It was derived for a Newtonian fluid by neglecting the effects due to curvature of the fluid film. This assumption is well justified as the effective radius of bearing components is generally very large compared with the film thickness. This enables the analysis to consider an equivalent curved surface near a plane.

The derivation of Reynolds equation involves the application of the basic equations of motion and continuity to the lubricant. The full equations of motion for a Newtonian fluid in Cartesian coordinates are:

$$\rho\frac{du}{dt}=\rho X-\frac{\partial p}{\partial x}+\frac{2}{3}\frac{\partial}{\partial x}\eta\left(\frac{\partial u}{\partial x}-\frac{\partial w}{\partial z}\right)+\frac{2}{3}\frac{\partial}{\partial x}\eta\left(\frac{\partial u}{\partial x}-\frac{\partial v}{\partial y}\right)$$

$$+\frac{\partial}{\partial y}\eta\left(\frac{\partial u}{\partial y}+\frac{\partial v}{\partial x}\right)+\frac{\partial}{\partial z}\eta\left(\frac{\partial u}{\partial z}+\frac{\partial w}{\partial x}\right) \qquad (2.1\text{ a})$$

$$\rho\frac{dv}{dt}=\rho Y-\frac{\partial p}{\partial y}+\frac{2}{3}\frac{\partial}{\partial y}\eta\left(\frac{\partial v}{\partial y}-\frac{\partial u}{\partial x}\right)+\frac{2}{3}\frac{\partial}{\partial x}\eta\left(\frac{\partial v}{\partial y}-\frac{\partial w}{\partial z}\right)$$

$$+\frac{\partial}{\partial z}\eta\left(\frac{\partial v}{\partial z}+\frac{\partial w}{\partial y}\right)+\frac{\partial}{\partial x}\eta\left(\frac{\partial v}{\partial x}+\frac{\partial u}{\partial y}\right) \qquad (2.1\text{ b})$$

$$\rho\frac{dw}{dt}=\rho Z-\frac{\partial p}{\partial z}+\frac{2}{3}\frac{\partial}{\partial z}\eta\left(\frac{\partial w}{\partial z}-\frac{\partial u}{\partial x}\right)+\frac{2}{3}\frac{\partial}{\partial z}\eta\left(\frac{\partial w}{\partial z}-\frac{\partial v}{\partial y}\right)$$

$$+\frac{\partial}{\partial x}\eta\left(\frac{\partial w}{\partial x}+\frac{\partial u}{\partial z}\right)+\frac{\partial}{\partial y}\eta\left(\frac{\partial w}{\partial y}+\frac{\partial v}{\partial z}\right) \qquad (2.1\text{ c})$$

The terms on the left hand side represent inertia effects and on the right hand side are the body force, pressure and viscous terms in that order. The inertia and body forces are negligible as compared to the viscous and inertia forces.

The equation of continuity representing conservation of mass is:

$$\frac{\partial\rho}{\partial t}+\frac{\partial\rho u}{\partial x}+\frac{\partial\rho v}{\partial y}+\frac{\partial\rho w}{\partial z}=0 \qquad (2.2)$$

The above Equations 2.la, 2.1b, 2.lc and 2.2, neglecting the relatively small valued terms like inertia and body force terms, pressure gradient across the film and introducing the values of the boundary velocities the following form of the Reynolds equation is obtained.

$$\frac{\partial}{\partial x}\left(\frac{\rho h^3}{12\eta}\frac{\partial p}{\partial x}\right)+\frac{\partial}{\partial z}\left(\frac{\rho h^3}{12\eta}\frac{\partial p}{\partial z}\right)=\frac{\partial}{\partial x}(phu) \qquad (2.3)$$

where $u=\frac{(u_1+u_2)}{2}$.

The second term in the above Equation (2.3) corresponds to side-leakage which refers to flow along z-direction. On neglecting the side-leakage term:

$$\frac{\partial}{\partial x}\left(\frac{\rho h^3}{12\eta}\frac{\partial p}{\partial x}\right)=\frac{\partial}{\partial x}(phu) \tag{2.4}$$

This equation is integrated to yield the familiar integrated form of Reynolds equation:

$$\frac{dp}{dx}=\frac{12\eta u}{\rho h^3}\left[(\rho h)-(\rho h)_e\right] \tag{2.5}$$

Where the subscript *e* refers to the conditions at the point where the pressure gradient *dp/dx* vanishes.

2.2.2 Elasticity equations

The lubricated contacting surfaces undergo elastic deformation due to which the pressure distribution and film shape are differing from the prediction of hydrodynamic lubrication theory. It is, therefore, important to evaluate the elastic displacements of the contacting surfaces. In the case of a line contact the pressure zone is very small compared with the radius of the solids. So the displacements are uniform along the length and the solids are in a condition of plane strain. The contact problem is usually simplified by calculating the displacements for a semi-infinite flat solid and adding to the curved surface of the roller.

The calculation begins from the Boussinesq function for the stresses due to a normal line load on the surface of a semi-infinite solid. The stresses and displacements under this line load can be integrated over the entire contact zone to give the corresponding quantities for a distributed pressure. The stress components in Cartesian co-ordinates are given as follows:

$$\sigma_x=-\frac{2Px^2y}{\pi\left(x^2+y^2\right)^2}$$

$$\sigma_y = -\frac{2Py^3}{\pi\left(x^2+y^2\right)^2}$$

$$\tau_{xy} = -\frac{2Pxy^2}{\pi\left(x^2+y^2\right)^2} \tag{2.6}$$

where P is the normal load per unit length

Using the relation between strain and stress components given by Hooke's law, the displacements u and v along x and y directions respectively, are obtained as follows:

$$u = \frac{\left(1-v^2\right)}{E}\int \sigma_x dx - \frac{v(1+v)}{E}\int \sigma_y\, dx + f(y) \tag{2.7a}$$

$$v = \frac{\left(1-v^2\right)}{E}\int \sigma_y dy - \frac{v(1+v)}{E}\int \sigma_x\, dy + g(x) \tag{2.7b}$$

where v is the Poisson's ratio

Using the above equations, the surface normal displacement, v , due to a pressure distribution $p(s)$ is given by

$$v(x) = \frac{\left(1-v^2\right)}{\pi E}\int_{s_1}^{s_2} p(s) In(x-s)^2\, ds + \text{constant} \tag{2.8}$$

where s_1 and s_2 mark the boundaries of the pressure zone

The integral in the above equation (2.8) cannot be solved by a straight forward numerical integration method because the integrand approaches minus infinity at x=s. Several workers used various methods to overcome this difficulty.

2.3 Advanced studies in EHL

Sternlicht et al. [28] could achieve convergence by using the finite difference forms of the governing equations. Archard et al. [29] described a useful approximate method, for the case of low-medium speed and high load, in which certain features were imposed on the pressure distribution.

Osterle and Stephenson [30] were successful in obtaining a converged solution for low loads. The processes mentioned above were based on straight iterations beginning with an assumed pressure distribution which was used to calculate deformation and film shape followed by the calculation of the new pressure distribution. But these processes were for only moderate loads and involved a large number of cycles of calculations.

The first significant results for practical loads were presented by Grubin [10]. Grubin's solution was based on two simplifying assumptions: (i) the deformed shape of the cylinders is the same as that in dry contact (ii) a high pressure is developed in the inlet region of the Hertzian zone. Based on his analysis Grubin derived an expression for film thickness

$$H_o = \frac{h_o}{R} = \frac{1.95(GU)^{8/11}}{W^{1/11}} \tag{2.12}$$

where, G, W and U are dimensionless material, load and speed parameters respectively, defined as:

$$G = \alpha E'.W = \frac{w}{E'R}.U = \frac{\eta_o u}{E'R} \tag{2.13}$$

α is the piezo-viscous coefficient of the lubricant.

The most important contribution was made by Dowson and Higginson [17] by presenting a numerical scheme applicable for a wide range of operating speeds and loads. Their analysis revealed several important facts which are outlined below:

(i) The minimum film thickness is much greater than predicted by simple theory.

(ii) In the range of operating conditions where elastic deformation is important, film thickness is only slightly dependent upon load.

(iii) The influence of the material parameter on the film thickness is almost as great as that of the speed parameter, but the practical range of the material parameter is small. So the speed parameter is the dominant variable.

(iv) The pressure distribution approaches towards the semi-elliptic Hertzian distribution for dry contact of the cylinders.

(v) For the conditions and materials encountered in the engineering practice there is usually a sharp secondary peak on the outlet side of the pressure distribution.

(vi) In pure rolling the friction force is independent of load and varies with the speed parameter at the same rate as does the film thickness.

(vii) At high loads the stress field in the solids is essentially Hertzian.

The most important outcome of this analysis was the derivation of the following formula for the minimum film thickness between rollers in EHL:

$$H_{\min} = \frac{h_{\min}}{R} = \frac{1.6G^{0.6}U^{0.7}}{W^{0.13}} \tag{2.14}$$

The above formula is used even today to get an estimate of the minimum film thickness under isothermal conditions.

2.4 Shear thinning effect

In order to understand the effect of the constitutive properties of lubricants, various rheological models have been investigated under heavily loaded EHL conditions.

The sinh-law based model often attributed to Ree and Eyring [31] is as follows:

$$\dot{\gamma} = \frac{du}{dy} = \frac{\tau_o}{\eta} \sinh\left(\frac{\tau}{\tau_o}\right) \tag{2.15}$$

Ree-Eyring fluid model has been very popular and used by Hirst and Moore [32], Johnson and Tevaarwerk [33], Berthe et al [34] and Johnson and Greenwood [35].

The full EHL solutions under isothermal conditions with Ree-Eyring fluid for various slides to roll ratios have been presented by Houpert and Hamrock [36], Conry et al [37] and Chang et al [38]. Houpert and Hamrock [36] reported no significant ifference in the film thickness between the Newtonian and non-Newtonian models for any slide/roll ratio. This is quite unexpected since all previous calculations for a non-Newtonian lubricant have reported some reduction in the film thickness. Houpert and Hamrock [36] argued that film thickness is established by hydrodynamic action in the inlet region alone and since the lubricant in the inlet region remains Newtonian for the range of speeds and loads considered, the non-Newtonian model gives identical film thicknesses to those by Newtonian model.

Similar results have been reported by Conry et al [37]. Hence, it is established that for pure rolling condition, the minimum film thickness should be independent of lubricant rheology.

Bair and Winer [39] proposed a well known form of non-linear constitutive equation where the limiting shear strength has been incorporated from the measurements of EHL experiments as:

$$\gamma = \frac{du}{dy} = \frac{1}{G_\infty}\frac{d\tau}{d\hat{t}} + \frac{\tau_L}{\eta} In\left(1-\hat{\tau}\right)^{-1} \tag{2.16}$$

Where, $\hat{\tau} = \tau/\tau_L$, τ_L =limiting shear strength.

Gecim and Winer [40] simplified the non-Newtonian fluid model of equation (2.16) as:

$$\gamma = \frac{du}{dy} = \frac{\tau_L}{\eta} \tanh(\hat{\tau}) \tag{2.17}$$

Using the above rheological model, Gecim and Winer [40] performed film thickness calculations and reported up to 40% reduction in film thickness below the corresponding values computed with Newtonian fluid model in rolling/sliding contacts. The first attempt to analyze the full solution of a non-Newtonian fluid model with the limiting shear strength in elastohydrodynamic lubrication was by Jacobson and Hamrock [41]. Moreover, the equations (2.16) and (2.17) are difficult to incorporate in the Reynolds equation. Iivonen and Hamrock [42] proposed a new and simpler rheological model as:

$$\gamma = \frac{du}{dy} = \frac{\tau_L}{\eta}\left[(1-\hat{\tau})^{-1} - 1\right] \tag{2.18}$$

It was further extended to the following general form [42]:

$$\gamma = \frac{du}{dy} = \frac{n\tau_L}{\eta}\left[(1-\hat{\tau})^{-1/n} - 1\right] \tag{2.19}$$

The above equation (2.19) is close to equation (2.16) when n is large. Therefore, it is more difficult to incorporate into Reynolds equation for large values of n. In order to overcome this problem Lee and Hamrock [43] proposed a more appropriate lubricant rheological circular model:

$$\gamma = \frac{du}{dy} = \frac{\tau_L \hat{\tau}}{\eta}\left(1-\hat{\tau}^2\right)^{-1/2} \tag{2.20}$$

A more generalized non-Newtonian fluid model [44, 45] in the form of power law has been used to represent the rheology of practical lubricants. It is given as:

$$\tau = \eta\left[\frac{du}{dy}\right]^{n-1}\frac{du}{dy} \tag{2.21}$$

Where, n is called as the power law index which is less than unity for shear thinning fluids and η is the reference viscosity. This fluid model has been used by several researchers in their recent works.

The combined effects of shear thinning and viscous heating on EHL characteristics of line contacts were described by Kumar and Khonsari [58]. A thermal EHL model was developed to simulate the combined effect of shear-thinning fluid behaviour and temperature rise of lubricant in rolling and sliding line contacts. Unlike the available studies on the combined effect of shear thinning and viscous heating using unrealistic non-Newtonian constitutive equations for near- Newtonian oils with low inlet viscosity, the present study employs the experimentally and theoretically proven Carreau model, which is applied to strongly shear-thinning oils with high inlet viscosity. An important feature of the present thermal EHL model is that the numerical scheme for Newtonian fluid can be applied without major changes. Some generalized models [2] are listed below in table 2.1

The Sinh law described in equation 2.15 was further modified by Kumar and Khonsari [57]. A concept of multiple flow units and relaxation time is added in this paper. Hence this is called Actual Ree Eyring model. The actual Ree-Eyring model is described by following equation

$$\tau = \sum_{i=1}^{N} x_i \tau_i \sinh^{-1}\left(\lambda_i \dot{\gamma}\right) \tag{2.22}$$

Where $\lambda_i = \frac{\mu}{\tau_i}$ is a characteristic or relaxation time, N is the number of flow units (N>1), x_i

Is a weighting fraction such that $\sum_{i=1}^{N} x_i = 1$ and μ is the low shear viscosity. The generalizedViscosity function is:

$$\eta = \frac{\tau}{\dot{\gamma}} = \sum_{i=1}^{N} x_i \frac{\tau_i}{\dot{\gamma}} \sinh^{-1}(\lambda_i \dot{\gamma}) \tag{2.23}$$

Table 2.1 Viscosity functions for the generalized Newtonian fluid model

$\eta(\dot{\gamma})$		$\eta(\tau)$	
$\eta = \mu$	Newtonian	$\eta = \mu$	Newtonian
$\eta = \mu\lvert\lambda\dot{\gamma}\rvert^{n-1}$	Ostwald-de waele	$\eta = \mu\lvert\tau/G\rvert^{1-\frac{1}{n}}$	Ostwald-deWaele
$\eta = \begin{cases} \mu, \lambda\dot{\gamma} \le 1 \\ \mu\lvert\lambda\dot{\gamma}\rvert^{n-1}, \lambda\dot{\gamma} \ge 1 \end{cases}$	Spriggs [19]	$\eta = \begin{cases} \mu, \tau/G \le 1 \\ \mu, \lvert\tau/G\rvert^{1-\frac{1}{n}}, \tau/G \ge 1 \end{cases}$	Sprigs [19]
$\eta = \mu_2 + \frac{\mu - \mu_2}{1 + \lvert\lambda\dot{\gamma}\rvert^{1-n}}$	Cross [6]	$\eta = \mu_2 + \frac{\mu - \mu_2}{1 + \left\lvert\frac{\tau}{G}\right\rvert^{\left(\frac{1}{n}-1\right)}}$	Ellis [7]
$\eta = \mu_2 + \frac{\mu - \mu_2}{\left[1 + (\lambda\dot{\gamma})^2\right]^{\frac{1-n}{2}}}$	Carreau [22]		
$\eta = \mu_2 + \frac{\mu - \mu_2}{\left[1 + (\lambda\dot{\gamma})^a\right]^{\frac{1-n}{a}}}$	Carreau-yasuda [3]	$\eta = \mu_2 + \frac{\mu - \mu_2}{1 + \left\lvert\frac{\tau}{G}\right\rvert}$	Ferry[20]
$\eta = \frac{\sum_{i=1}^{N} \frac{f_i \mu}{\lambda_i \dot{\gamma}} \sinh^{-1}(\lambda_i \dot{\gamma})}{\sum_{i=1}^{N} f_i = 1, N > 1}$	Ree-Eyring [25]	$\eta = \mu_2 + \frac{\mu - \mu_2}{1 + \left(\frac{\tau}{G}\right)^2}$	Rabinowitsch [21]
		$\eta = \mu_2 + \frac{\mu - \mu_2}{\left[1 + \left(\frac{\tau}{G}\right)^a\right]^{\frac{\frac{1}{n}-1}{a}}}$	Bair [23-24]

Chapter 3

ANALYSIS

3.1 Introduction

The contacts in mechanical components, such as gears, roller bearings and cams are simulated by EHL line contacts. The extensive review of the relevant literature, presented in Chapter 2, includes the shear thinning effects in EHL and advanced studies in this field. Therefore, the present study attempts to investigate the shear thinning effects by the use of Ree-Eyring model in EHL contacts with the consideration of different number of flow units. This chapter describes the mathematical model employed in the present study.

3.2 Numerical model

The analysis of elastohydrodynamic lubrication of line contacts, as shown in Fig 3.1, involves the simultaneous solution of Reynolds equation, elasticity equation and load equilibrium equation subject to appropriate boundary conditions with due consideration to the variation of the fluid properties - viscosity and density, with pressure. Therefore, the following subsections present a detailed description of the governing equations.

3.2.1 Actual Ree Eyring Model

The viscosity-shear strain rate relationship proposed by Ree and Eyring [57] has been used because it covers EHL behaviour of shear thinning lubricants. The generalized viscosity function is given by:

$$\eta = \frac{\tau}{\dot{\gamma}} = \sum_{i=1}^{N} x_i \frac{\tau_i}{\dot{\gamma}} \sinh^{-1}\left(\lambda_i \dot{\gamma}\right) \tag{3.1}$$

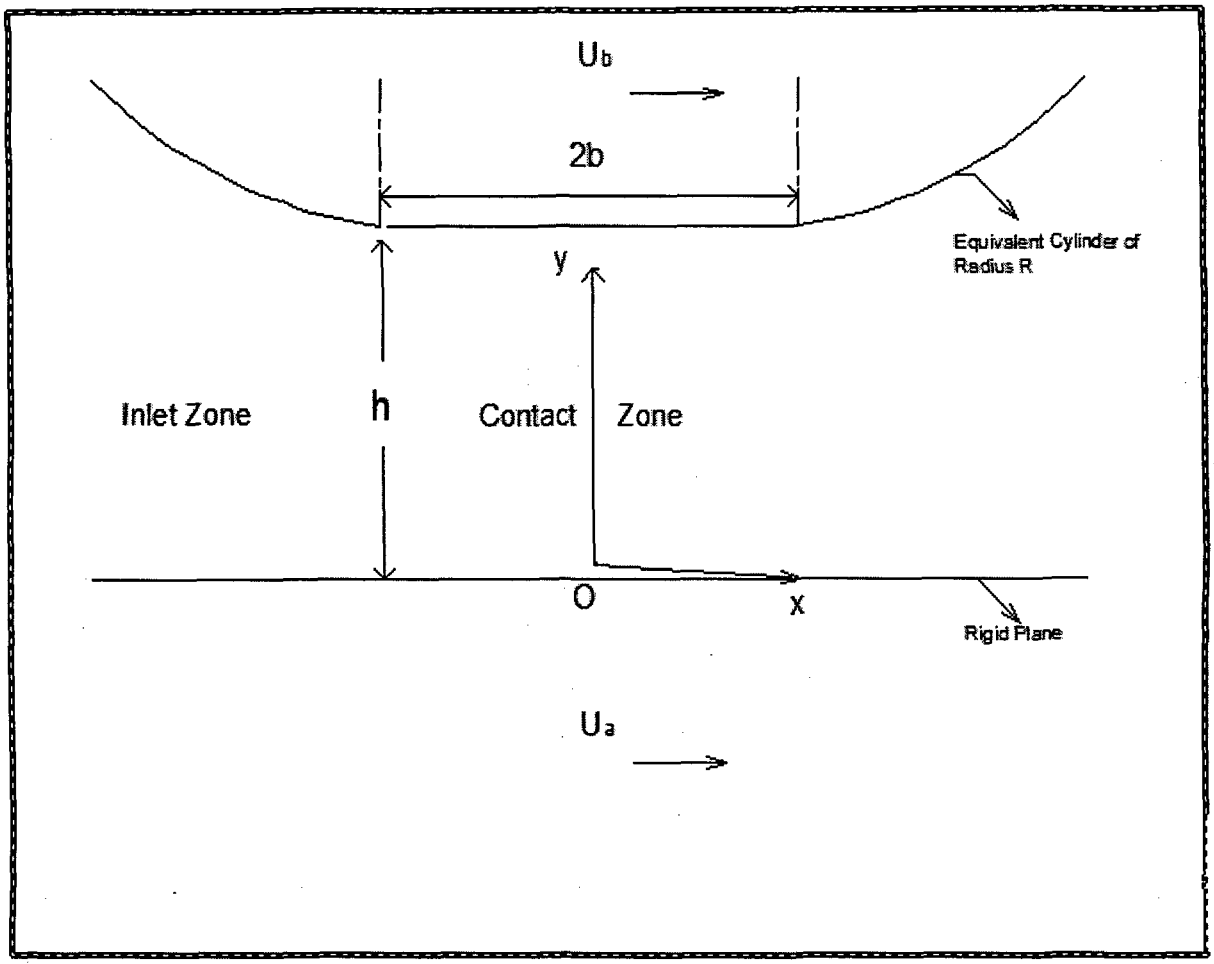

Fig 3.1 Contact geometry and co-ordinate axes

3.2.2 Velocity and Velocity Gradient

The fluid velocity distribution along the rolling direction is given below in dimensional form

$$u = u_a + \frac{(u_b - u_a)}{h} y + \frac{(y^2 - hy)}{2\eta'} \frac{\partial p}{\partial x} \tag{3.2}$$

The velocity gradient along the film is given by:

$$\frac{\partial u}{\partial y} = \frac{(u_b - u_a)}{h} + \frac{(2y - h)}{2\eta'} \frac{\partial p}{\partial x} \tag{3.3}$$

where η' is the effective lubricant viscosity derived using perturbation method described subsequently.

3.2.3 Reynolds equation

The fluid pressure at the inlet as well as the outlet of an EHL conjunction is equal to the ambient pre sure [55, 56]. In addition, the decline of pressure to the ambient value at the outlet is gradual, which implies that the pressure gradient at the outlet approaches zero. Based upon the assumptions used by Dien and Elrod [59], several researchers use a perturbation scheme to derive a modified Reynolds equation incorporating the effect of non-Newtonian lubricant behavior. The basic methodology used in a perturbation scheme is shown below for the case of a line contact. The scheme begins with the introduction of equivalent viscosity, η_e, which is given by

$$\eta_e = \tau / I \tag{3.4}$$

where $I = \partial u / \partial y$. Now, velocity u is expanded in terms of ε, which is a small non-dimensional amplitude parameter:

$$u = u_0 + \varepsilon u_1 \tag{3.5}$$

Then

$$I = I_0 + \varepsilon I_1 \tag{3.6}$$

$$\text{where } I_0 = \frac{\partial u_0}{\partial y}, I_1 = \frac{\partial u_1}{\partial y} \tag{3.7}$$

Expanding the equivalent viscosity η_e in the region near I_0 into a Taylor series:

$$\eta_e = \eta_0 + \varepsilon \eta_1 \tag{3.8}$$

where

$$\eta_0 = \eta_e(I_0) \text{ and } \eta_1 = I_1\left(\frac{\partial \eta_e}{\partial I}\right)_{I_0} \tag{3.9}$$

The momentum equation is:

$$\frac{\partial \tau}{\partial y} = \frac{\partial p}{\partial x} \tag{3.10}$$

Using Equations (3.7), (3.6), (3.8) and neglecting ε^2:

$$\tau = (\eta_0 + \varepsilon \eta_1)(I_0 + \varepsilon I_1) = \eta_0 I_0 + \varepsilon(\eta_1 I_0 + \eta_0 I_1) \tag{3.11}$$

Expanding p,

$$p = 0 + \varepsilon\, p' \tag{3.12}$$

Substituting Equations (3.11) and (3.12) in Equation (3.10):

$$\eta_0 \frac{\partial I_0}{\partial y} + \varepsilon \frac{\partial(\eta_1 I_0 + \eta_0 I_1)}{\partial y} = \varepsilon \frac{\partial p'}{\partial x} \tag{3.13}$$

$$\Rightarrow \quad \eta_0 \frac{\partial^2 u_0}{\partial y^2} = 0 \tag{3.14}$$

$$\text{And} \quad \frac{\partial(\eta_1 I_0 + \eta_0 I_1)}{\partial y} = \frac{\partial p'}{\partial x} \tag{3.15}$$

Integrating Equation (3.14) under the boundary conditions, $u_0 = u_a$ at $y = 0$ and $u_0 = u_b$ at $y = h$:

$$u_0 = u_a + \frac{(u_b - u_a)}{h} y \tag{3.16}$$

Where u_a, u_b are the velocities of the lower and upper surfaces respectively and h is the

film thickness. Substituting Equation (3.9) into Equation (3.15) gives

$$\eta' \frac{\partial^2 u_1}{\partial y^2} = \frac{\partial p'}{\partial x} \tag{3.17}$$

$$\text{where, } \eta' = \left(I_0 \left(\frac{\partial \eta_e}{\partial I} \right)_{I_0} + \eta_0 \right) \tag{3.18}$$

Integrating Equation (3.17) under the boundary conditions, $u_1 = 0$ at $y = 0$ and $u_1 = 0_b$ at $y = h$

$$u_1 = \frac{\left(y^2 - hy\right)}{2\eta'} \frac{\partial p'}{\partial x} \tag{3.19}$$

From Equations (3.5), (3.12), (3.16) and (3.18)

$$u = u_a + \frac{\left(u_b - u_a\right)}{h} y + \frac{\left(y^2 - hy\right)}{2\eta'} \frac{\partial p}{\partial x} \tag{3.20}$$

$$\frac{\partial u}{\partial y} = \frac{\left(u_b - u_a\right)}{h} + \frac{\left(2y - h\right)}{2\eta'} \frac{\partial p}{\partial x} \tag{3.21}$$

Applying the above perturbation scheme to actual Ree-Eyring model:

$$\eta_e = \tau / \dot{\gamma} = \sum_{i=1}^{N} x_i \frac{\tau_i}{\dot{\gamma}} \sinh^{-1}\left(\lambda_i \dot{\gamma}\right) \tag{3.22}$$

$$\frac{\partial \eta_e}{\partial I} = \sum_{i=1}^{N} x_i \left[\frac{\tau_i}{I} \frac{\lambda_i}{\sqrt{1 + \left(\lambda_i I\right)^2}} - \frac{\tau_i}{I^2} \sinh^{-1}\left(\lambda_i I\right) \right] \tag{3.23}$$

$$\eta' = \left(I_0 \left(\frac{\partial \eta_e}{\partial I} \right)_{I_0} + \eta_0 \right) = \mu \sum_{i=1}^{N} \frac{x_i}{\sqrt{1 + \left(\mu \frac{u_b - u_a}{h \tau_i} \right)^2}} \tag{3.24}$$

Therefore, modified Reynolds equation is:

$$\frac{\partial}{\partial x}\left(\frac{\rho h^3 \partial p/\partial x}{12\xi\mu}\right)=u_o\frac{\partial}{\partial x}(\rho h) \tag{3.25}$$

where

$$\xi=\sum_{i=1}^{N}\frac{x_i}{\sqrt{1+\left(\mu\frac{u_b-u_a}{h\tau_i}\right)^2}}$$

In dimensionless form:

$$\frac{\partial}{\partial X}\left(\frac{\bar{\rho}H^3\partial P/\partial X}{\xi\bar{\mu}}\right)=K\frac{\partial}{\partial X}(\bar{\rho}H) \tag{3.26}$$

$$\xi=\sum_{i=1}^{N}\frac{x_i}{\sqrt{1+\left(\frac{\pi SUE'\bar{\mu}}{8WH\tau_i}\right)^2}} \tag{3.27}$$

$$\tau=\left[\sum_{i=1}^{N}x_i\frac{\tau_i}{\dot{\gamma}}\sinh^{-1}(\lambda_i\dot{\gamma})\right]\left[\frac{(u_b-u_a)}{h}+\frac{(2y-h)}{2\eta'}\frac{\partial p}{\partial x}\right] \tag{3.28}$$

$$\tau(y=h)=\left[\sum_{i=1}^{N}x_i\tau_i\sinh^{-1}\left(\frac{\mu}{\tau_i}\frac{(u_b-u_a)}{h}+\frac{h}{2\tau_i\xi}\frac{\partial p}{\partial x}\right)\right] \tag{3.29}$$

In dimensionless form:

$$\bar{\tau}(y=h)=\left[\sum_{i=1}^{N}x_i\frac{\tau_i}{E'}\sinh^{-1}\left(\frac{\pi SUE'\bar{\mu}}{8WH\tau_i}+\frac{WHE'}{\pi\tau_i\xi}\frac{\partial P}{\partial X}\right)\right] \tag{3.30}$$

Inlet boundary condition

$$P=0 \text{ at } X=X_{in} \tag{3.31}$$

Outlet boundary condition

$$P = \frac{\partial P}{\partial X} = 0 \ at \ X = X_0 \tag{3.32}$$

3.2.4 Finite difference formulation

The Reynolds equation is discretized by using a finite differencing scheme to obtain the equations $f_i = 0$ (2 to N) as follows:

$$f_i = \varepsilon_{i+1/2} \frac{P_{i+1} - p_i}{\Delta X^2} - \varepsilon_{i-1/2} \frac{P_i - p_{i-1}}{\Delta X^2} - K \frac{\left[\left(\overline{\rho H}\right)_i - \left(\overline{\rho H}\right)_{i-1}\right]}{\Delta X} \tag{3.33}$$

where $\varepsilon_i = \left(\frac{\overline{\rho} H^3}{\overline{\mu} \xi}\right)_i$

3.2.5 Boundary conditions

Since the first node lies at $X = X_{in}$, P_1 is kept fixed at 0 in order to satisfy the inlet boundary condition imposed by equation (3.32). The outlet boundary coordinate X_o is determined by following a procedure in which Xo is initially set equal to the maximum value of X -coordinate, X_{max}, used in the numerical simulation. The new values of pressure are calculated. X_N is then located such that $P < 0$ for $X > X_N$, where X_N represents the X-coordinate of the node nearest to X_o and $X_N < X_o$. P_{N-1}, where P_N and P_{N+1} are used to define a second degree polynomial $P(X)$ as follows:

$$P(X) = AX^2 + BX + C \tag{3.34}$$

where A, B, C are unknown constants to be determined by solving the following equations:

$$AX_{N-1}^2 + BX_{N-1} + C = P_{N-1}$$

$$AX_N^2 + BX_N + C = P_N$$

$$AX_{N+1}^2 + BX_{N+1} + C = P_{N+1} \tag{3.35}$$

The solution of the above equations gives

$$A = \frac{(P_{N-1} + P_{N-1} - 2P_N)}{2(\Delta X)^2}$$

$$B = \frac{(P_{N+1} - P_{N-1})}{2(\Delta X)} - X_N \frac{(P_{N-1} + P_{N+1} - 2P_N)}{(\Delta X)^2}$$

$$C = X_N^2 \frac{(P_{N-1} + P_{N+1} - 2P_N)}{2(\Delta X)^2} - X_N \frac{(P_{N+1} + P_{N-1})}{2(\Delta X)} + P_N \tag{3.36}$$

X_0 is calculated such that $P(X_0) = 0$,

$$AX_0^2 + BX_0 + C = 0 \tag{3.37}$$

The new value of X_N is given by the X-coordinate of the node nearest to the outlet boundary defined by the above equation (3.37) such that X_N and X_0. After a few iterations X_0 and X_N attain steady values.

3.2.6 Film thickness equation

The film thickness, h, at any point in a rough EHL conjunction is:

$$h = h_0 + \frac{x^2}{2R} + v \tag{3.38}$$

Where h_0 is the offset film thickness, v contributes to the surface normal displacement and the method adopted for its calculation is discussed subsequently.

The film thickness in non-dimensional form is given by:

$$H(X) = H_0 + \frac{X^2}{2} + \bar{v} \tag{3.39}$$

where, $\bar{v} = vR/b^2$ is the non-dimensional surface displacement.

3.2.7 Elastic deformation

The elasticity integral is expressed in non-dimensional form [48] as follows:

$$\bar{v} = \frac{1}{2\pi} \int_{X_{in}}^{X_0} P \, In(X - S)^2 \, dS \tag{3.40}$$

The above equation is represented in discrete form as follows:

$$\bar{v}_i = \sum_{j=1}^{N} D_{ij} P_j \tag{3.41}$$

where, D_{ij} is the influence coefficient at node i due to a unit pressure at node j.

Venner et al [55] used a simple expression for influence coefficients for evaluation of elastic deformation in EHL line contacts. This expression, as given below, is applicable when a uniform mesh is used for discretization:

$$D_{ij} = \frac{1}{\pi}\left[\left(i - j + \frac{1}{2}\right)\Delta X\left\{In\left(\left|i - j + \frac{1}{2}\right|\Delta X\right) - 1\right\}\right.$$

$$\left. -\left(i - j - \frac{1}{2}\right)\Delta X\left\{In\left(\left|i - j - \frac{1}{2}\right|\Delta X\right) - 1\right\}\right] \tag{3.42}$$

where ΔX is the grid size of the uniform mesh used.

The non-dimensional elastic deformation computed from above equation (3.40) is used for the calculation of fluid film thickness, which is required for the calculation of pressures.

3.2.8 Density-Pressure Relationship

The present analysis uses Dowson and Higginson [3] density-pressure relationship for the lubricant in the dimensionless form:

$$\bar{\rho} = \left(1 + \frac{0.6 \times 10^{-9} P.p_h}{1 + 1.7 \times 10^{-9} P.p_h}\right) \tag{3.43}$$

3.2.9 Viscosity-Pressure Relationship

The present analysis uses the following relation for viscosity in the dimensionless form:

$$\bar{\mu} = \exp\left[\left(In\mu_0 + 9.67\right)\left\{-1 + \left(1 + 5.1 \times 10^{-9} P.p_h\right)^z\right\}\right] \tag{3.44}$$

3.2.10 Load Equilibrium Equation

The pressure developed in the lubricant supports the applied load. Therefore, the pressure distribution obtained from the Reynolds equation should satisfy the following condition

$$\int_{x_i}^{x_a} p dx = w \tag{3.45}$$

where w is the applied load per unit width. The above equation is expressed in non-dimensional form as follows:

$$\int_{x_i}^{x_a} p dX = \frac{\pi}{2} \tag{3.46}$$

The integral in equation (3.46) is calculated using Simpson's rule and it can be written in the following form:

$$\Delta W = \sum_{j=2}^{N} C_j P_j - \frac{\pi}{2} = 0 \tag{3.47}$$

$$\text{where, } C_j = \begin{cases} \Delta X/3 & j = 1 \\ 4\Delta X/3 & j = 2,4,6... \\ 2\Delta X/3 & j = 3,5,7... \end{cases} \tag{3.48}$$

3.2.11 Newton-Raphson Formulation

The simultaneous system of N equations by discretized Reynolds equation (3.33) and discretized load equilibrium equation (3.48) are solved using the Newton-Raphson technique. The N system unknowns are P_2, $P_3, P_4, ..., P_N$ and H_0. The matrix equation of this system is

$[J]\ [\Delta] = [F]$, i.e.

$$\begin{bmatrix} \frac{\partial f_2}{\partial P_2} & \frac{\partial f_2}{\partial P_3} & \cdots & \frac{\partial f_2}{\partial P_N} & \frac{\partial f_2}{\partial H_0} \\ \frac{\partial f_3}{\partial P_2} & \frac{\partial f_3}{\partial P_3} & \cdots & \frac{\partial f_3}{\partial P_N} & \frac{\partial f_3}{\partial H_0} \\ \cdots & \cdots & \cdots & \cdots & \cdots \\ \vdots & \vdots & \vdots & \vdots & \vdots \\ \frac{\partial f_N}{\partial P_2} & \frac{\partial f_N}{\partial P_3} & \cdots & \frac{\partial f_N}{\partial P_N} & \frac{\partial f_N}{\partial H_0} \\ C_2 & C_3 & \cdots & C_N & 0 \end{bmatrix} \begin{bmatrix} \Delta P_2 \\ \Delta P_3 \\ \cdots \\ \cdots \\ \Delta P_N \\ \Delta H_0 \end{bmatrix} = - \begin{bmatrix} f_2 \\ f_3 \\ \cdots \\ \cdots \\ f_N \\ \Delta W_0 \end{bmatrix} \tag{3.49}$$

The elements of the Jacobian matrix $[J]$ are calculated as described in Appendix 1.

3.2.12 Coefficient of friction

The coefficient of friction is taken as the ratio of total shear force of the lubricant at the surface boundaries and the applied normal load as expressed by the following equation

$$COF = \frac{\int_{x_i}^{x_o} \tau(y=0)\,dx}{w} \tag{3.50}$$

Chapter-4

SOLUTION PROCEDURE

4.1 Introduction

The preceding chapter describes the governing equations for the analysis of the Ree-Erying model for shear thinning lubricants in elastohydrodynamic lubrication. A computer program is developed and the solution procedure is adopted for the numerical implementation of the governing equations, are described in this chapter.

The primary aim of the computer program is to determine the pressure distribution and fluid profile within the EHL contact. Therefore, pressure, minimum film thickness, central film thickness and coefficient of friction are the primary variables which are calculated by using the secondary variables namely fluid viscosity, density and elastic deformation. It is apparent from the nature of the governing equations that the above mentioned primary and secondary variables are interdependent. For example, pressure is calculated from Reynolds equation by using film thickness, viscosity and density; the film thickness depends upon elastic deformation which is calculated by using the pressure distribution.

4.2 Overall Solution Procedure

The steps involved in the overall solution scheme are given below

1. The pressure distribution $[P]$, offset film thickness H_0 and outlet boundary co-ordinate X_o are initialized to some reference values.
2. The current distribution is used to calculate surface displacements $[\bar{v}]$ using equation (3.41).
3. The surface displacement $[\bar{v}]$ are used along with the offset film thickness H_o to evaluate the fluid film thickness, at every node by using film thickness equation (3.39)

4. The fluid density ($\bar{\rho}$) and viscosity ($\bar{\mu}$) are calculated using equation (3.43) and (3.44) respectively.
5. This step executes the calculation of viscosity modification factor ξ given by equation (3.27).
6. The residual vector $[f]$ is calculated from equation (3.33).
7. The residual vector ΔW is calculated from the load equilibrium equation (3.47).
8. The residual vectors calculated in the steps 6 and 7 are assembled in a single vector $[F]$ to facilitate execution of Newton-Raphson scheme.
9. This is followed by computation of Jacobian coefficients, as described in Appendix-1, to get the Jacobian matrix $[J]$.
10. The corrections to the system variables, specified by vectors on the left hand side of equation (3.49) are computed by inverting the Jacobin matrix using Gauss elimination.
11. The corrections calculated in step 10, are added to the corresponding system variables to get the new values of pressure distribution and offset film thickness.
12. The outlet boundary co-ordinate X_0 is corrected by using equations (3.36) and (3.37).
13. The X-coordinate of the node nearest to the outlet boundary is set equal to X_N such that $X_N < X_o$. This decides the number of nodes N in the solution domain.
14. The pressure gradients along the fluid film are calculated. The termination of the iterative loops in the EHL analysis of line contacts requires the fulfilment of the predefined convergence criteria to arrive at an accurate solution. In order to check the convergence of the pressure distribution, the sum of the nodal pressures corresponding to the current iteration (say nth) is calculated. If the fractional difference between this value and that corresponding to the previous iteration is less than the prescribed tolerance TOL, the pressure distribution is assumed to have converged. Thus,

$$\frac{\left|\left[\sum_{i=1}^{N} P_i\right]_n - \left[\sum_{i=1}^{N} P_i\right]_{n-1}\right|}{\left|\left[\sum_{i=1}^{N} P_i\right]_{n-1}\right|} \leq TOL \tag{4.1}$$

The offset film thickness is assumed to converge if the fractional change in its value becomes less than the prescribed tolerance in successive iterations

$$\frac{\left|[H_o]_n - [H_0]_{n-1}\right|}{|H_o|_{n-1}} \leq TOL \tag{4.2}$$

The value of TOL adopted in the analysis is 1×10^{-4} as it has been found that a lower value does not contribute to improve the accuracy of the solution. The iterative loop terminates and the current values are considered as the final solution only if all the relevant convergence criteria are satisfied simultaneously.

15. If any one or more of the relevant criteria are not satisfied, the next iteration begins and the control is shifted back to the step 2.

Chapter 5

RESULTS AND DISCUSSION

5.1 Introduction

The previous chapters described the EHL model and the solution procedure which are applied in this chapter for the evaluation of EHL characteristics with actual Ree-Eyring model to describe the shear-thinning behavior in line contacts. The EHL simulation results are presented and the suitability of actual Ree Eyring model for EHL lubricants is discussed in the sections to follow.

5.2 Influence of Lubricant Rheology in EHL

Tables 5.1 and 5.2 show the Ree-Eyring parameters for different oils used in present work and the output parameters to be studied respectively.

Sr.N.	Lubricant	N	x_1	x_2	x_3	τ_1(MPa)	τ_2(MPa)	τ_3(MPa)	Ref.
1	LF 5346	2	0.876	0.124	-	0.00917	2	-	[57]
2	PG 460	2	0.676	0.324	-	0.0164	3.9	-	[62]
3	LF 5346	3	0.791	0.147	0.062	0.00519	0.23	11.02	[57]
4	PDMS	3	0.781	0.147	0.072	0.00519	0.23	25	[57]

Table 5.1 Actual Ree-Eyring parameters for different oils

It may be noted that for the case of LF 5346 gear oil, Table 5.1 includes two sets of Ree-Eyring parameters which correspond to 2 and 3 flow units in the constitutive equation. Also, it needs a mention that the lubricants used in the present analysis differ only in terms of rheology while the piezo-viscous properties are kept fixed so as to avoid alteration of the rheological effect characteristics due to superposition of different piezo-viscous behaviors.

S. No.	Input Parameters	Output Characteristics
1	Dimensionless load (W=2x10^{-5} to 5x10^{-4})	Dimensionless Minimum Film Thickness
2	Dimensionless speed (U=5x10^{-12} to 5x10^{-10})	Dimensionless Central Film Thickness
3	Slide to roll ratio(0 to2)	Pressure Distribution
4	Ree-Eyring parameters: N, τ_i and x_i	Coefficient of friction (COF) vs. S

Table 5.2 Output characteristics to be studied

\5.2.1 Comparison of lubricant rheology

Figure5.1 compares the variations of generalized Newtonian viscosity (η) with shear-rate obtained using actual Ree-Eyring model with 2 and 3 flow units, sinh law [62] and the well established Carreau model [59] for the case of LF 5346 gear oil. The "sinh law" refers to the popular form of Ree-Eyring model with only one flow unit. It can be seen from Figure 1 that there is a good agreement between the actual Ree-Eyring and Carreau models. However, as reported by Bair [62], at high shear-rates, the actual Ree-Eyring model predicts a much steeper drop in the effective lubricant viscosity and hence, a more pronounced shear-thinning effect as compared to the Carreau model which is known to replicate experimental flow behaviour most accurately. This departure from Carreau model can be minimized by increasing the number of flow units as apparent from Fig 5.1. Further, it may be noted that the most widely used sinh law either underestimates or overestimates the shear-thinning effect to a great extent.

Similarly, Figures5.2 and 5.3 displays the flow curves obtained using Carreau [59] and actual Ree-Eyring models for PG 460 and PDMS oils respectively. It may be noted that, unlike LF 5346 and PG 460, the Ree-Eyring parameters of PDMS oil are such that the deviation of Ree-Eyring viscosity from the corresponding Carreau viscosity is more evenly distributed between low and high shear rates to avoid overestimation of shear-thinning behaviour at high shear-rates typically encountered in EHL inlet zone.

5.2.2 Effect of Load

Figure5.4 compares the variation of dimensionless minimum film thickness i.e. h_{min}/R with dimensionless load parameter for different oils i.e. LF5346 gear oil, PG 460 and PDMS oil at a constant rolling velocity u=0.1 *m/s* and slide to roll ratio S=1. It can be seen that h_{min}/R decreases with increasing value of W as expected. The minimum film thickness pertaining to LF 5346 gear oil does not vary appreciably with increase in the number of flow units from 2 to 3. This indicates that under the present operating conditions two flow units in the Ree-Eyring model are sufficient to model the shear-thinning behaviour of LF 5346 gear oil. Further, it can be seen that the minimum film thickness values for LF 5346 gear oil are slightly lower than the corresponding values for PDMS oil, while those for PG 460 oil are much higher. Similar trends can be seen in Figure5.5 which shows the variation of dimensionless central film thickness with load parameter. These observations, in consonance with the $\eta - \dot{\gamma}$ curves (Figures 5.1 – 5.3), indicates that LF 5346 gear oil is the most shear-thinning lubricant of the three oils, whereas, PG 460 oil exhibits a much less pronounced shear-thinning effect.

Recently, it has been proved experimentally as well as theoretically that the EHL film thickness for shear-thinning lubricants is more sensitive to maximum Hertzian pressure (p_H) and hence, load as compared to Newtonian fluids. The sensitivity of EHL film thickness to maximum Hertzian pressure may be obtained by evaluating the slope of $\log(h_{\min}/R) - \log p_H$ (or $\log(h_c/R) - \log p_H$) characteristics. In the present work, the actual Ree-Eyring model has been used for the first time in order to capture this effect.

Table 5.3 shows the sensitivities of minimum and central film thickness to p_H for the three oils under consideration. It can be seen that the film thickness sensitivities to p_H increase with increasing shear-thinning behaviour of three oils.

Oils	h_{min}/R		h_c/R		$\left\|\frac{d\log(h_{min}/R)}{d\log(p_H)}\right\|$	$\left\|\frac{d\log(h_c/R)}{d\log(p_H)}\right\|$
	p_H=0.4 (GPa)	p_H=1.094 (GPa)	p_H=0.4 (GPa)	p_H=1.094 (GPa)		
PG 460	5.49×10^{-6}	4.08×10^{-6}	6.77×10^{-6}	4.83×10^{-6}	0.147366	0.16670
PDMS	2.09×10^{-6}	1.49×10^{-6}	2.66×10^{-6}	1.83×10^{-6}	0.16678	0.18652
LF 5346	1.99×10^{-6}	1.41×10^{-6}	2.55×10^{-6}	1.73×10^{-6}	0.171459	0.19140

Table 5.3 Film thickness sensitivity to maximum Hertzian pressure (load)

Figure5.6 shows the variation of coefficient of friction (COF) with dimensionless load parameter for the three oils under investigation at u=0.1 *m/s* and S=1. It can be seen that COF increases with increasing value of W, however, with a decreasing rate due to increasing shear-thinning effect at higher loads. It is interesting to note that the coefficient of friction for PDMS oil is higher than that for PG 460 oil even though the former exhibited more pronounced shear-thinning effect as compared to the latter in Figures 5.4 and 5.5. In this regard, it is important to understand the factors that determine friction in an EHL contact. The shear stress ensuing in the EHL contact zone due to lubricant viscosity and shear-strain rate governs the coefficient of friction. As PDMS oil is more shear-thinning, its viscosity is lower than that of PG 460 oil. However, on account of thinner film, the shear-strain rate for PDMS oil is high enough to outweigh

the effect of lower viscosity and hence, higher COF values as compared to PG 460 oil. On the other hand, as evident from Figure 5.6, the shear-thinning effect on the viscosity of LF 5346 gear oil is so pronounced that the compensating effect of thinner fluid film (higher shear-strain rate) fails to play a decisive role and therefore, LF 5346 gear oil yields minimum values of COF. Further, it may be noted that, unlike film thickness, there is a significant difference in the COF values obtained using 2 and 3 flow units in the Ree-Eyring model. Therefore, it may be concluded that using lesser number of flow units underestimates the value of coefficient of friction.

Figure5.7 compares the pressure distribution at two different loads $W=1\times10^{-4}$ and 5×10^{-5} for LF 5346 and PG 460 oils. The rolling speed and slide to roll ratio are kept fixed at 0.1m/s and 1 respectively. It can be seen that the pressure distribution at higher load is closer to the parabolic Hertzian distribution for dry contact.

5.2.3 Effect of slide to roll ratio

Figures 5.8 and 5.9 compare the variation of h_{min}/R and h_c/R respectively with slide to roll ratio, S, for the three oils at u=0.1 *m/s* and W=1.3x10^{-4}. It can be seen that the minimum and central film thickness decrease with increasing slide to roll ratio for all the three oils. This is due to the fact that shear rate increases with increasing slide to roll ratio which, in turn, leads to more pronounced decrease in lubricant viscosity on account of shear-thinning behaviour. As PG 460 oil is the least shear-thinning of the three oils, its film thickness decreases at a gradual rate as compared to the other two oils (PDMS and LF 5346), which exhibit a major drop in film thickness values for a small increase in slide to roll ratio from 0 to around 0.2. Also, as apparent from the curves pertaining to LF 5346 gear oil, it is reconfirmed that using 2 flow units in the Ree-Eyring model is sufficient from the viewpoint of film thickness prediction.

Figure 5.10 compares the COF-S characteristics for the three test oils at u=0.1 *m/s* and W=1.3x10^{-4}. It can be seen that for pure rolling, i.e. S=0, all the oils have minimum

coefficient of friction and as the slide to roll ratio increases, COF also increases. The magnitude of COF for the three oils follows the same order as in Figure 5.6 and the same reasoning applied here as well.

5.2.4 Effect of speed

Figures5.11 and 5.12 compare the variations of h_{min}/R and h_c/R with dimensionless speed parameter, U, for the three oils under consideration at S=1 and W=1.3×10^{-4}. It can be seen that minimum as well as central film thicknesses increase with increasing speed parameter as expected. However, as the shear-thinning effect increases (in the order PG 460, PDMS and LF 5346), the slope of the curves decreases. Also, it can be seen that the film thickness values for the case of LF 5346 gear oil using 2 and 3 flow units are close to each other only at very low values of U. This is an important observation and it calls for the modification of the statement made earlier - using 2 flow units for a highly shear-thinning lubricant may be sufficient for film thickness prediction at low speeds only. The deviation from the usual linear trend of the film thickness curves pertaining to LF 5346 gear oil with 2 flow units in Figures 5.11 and 5.12 further indicates the inadequacy of 2 flow units for this oil. This can be explained on the basis of $\eta - \dot{\gamma}$ curve for the case of LF 5346 with 2 flow units (Figure 5.1) showing highly pronounced shear-thinning effect at high shear rates (and hence, high speeds) as compared to actual (Carreau model). Furthermore, it needs a mention that the slope of the $h-U$ curve on log-log scale reflects the sensitivity of EHL film thickness to the operating speed and it is known to be around 0.7 for a lubricant which remains Newtonian in the inlet zone. However, in agreement with the observations of several researchers, the slopes of these curves for all the three non-Newtonian oils considered here are below 0.6. This further establishes the validity of Ree-Eyring model and the numerical algorithm employed here.

Figure5.13 shows the variation of coefficient of friction with dimensionless speed parameter for the three oils at W=1.3×10^{-4} and S=1. It can be seen from the figure that the coefficient of friction for all three oils increases slightly with increasing value of U and

then exhibits a marginally decreasing or almost constant value. The decreasing trend is most pronounced in the case of PG 460 oil. As explained earlier, COF depends upon lubricant viscosity and the operating shear rate in the EHL contact zone. The lubricant viscosity itself, on account of shear-thinning behaviour, depends on shear rate, which is a function of speed and film thickness. An increase in operating speed causes an increase in shear rate; however, as higher speed is also associated with thicker fluid films, the overall increase in the shear rate and hence, COF is limited. The lubricant viscosity, on the other hand, tends to decrease with increasing speed due to enhanced shear-thinning effect. Therefore, the variation of COF with U is governed by the superposition of these intercoupled effects.

5.2.5 Effect of radius

Conventionally, EHL characteristics are studied with respect to dimensionless operating parameters as in the previous three subsections. However, it has been discovered only recently that the scale sensitivity of EHL film thickness is higher for shear-thinning fluids is much higher as compared to Newtonian. Therefore, EHL film thickness pertaining to shear-thinning fluids changes by a larger proportion on an increase or decrease in the radius. In other words, shear-thinning effect has been found to be more pronounced at smaller radius. This is due to higher shear rates attributed to thinner films and relatively rapid filling of inlet zone leading to higher pressure gradient at smaller radius. These factors result in a higher shear stress within the EHL inlet zone and hence, a more pronounced shear-thinning effect. As it is an important fact and it is necessary to check if the rheological model used to describe the shear-thinning behaviour can capture this effect. Therefore, Figures 5.14 and 5.15 compare the variation and minimum a central film thickness respectively, with radius for the three oils under investigation. It can be seen that the scale sensitivities of minimum as well as central film thicknesses, given by the slopes of h_{min}–R and h_c–R curves plotted on log-log scale, increase in the order of increasing shear-thinning behaviour, i.e., PG 460, PDMS and LF 5346.

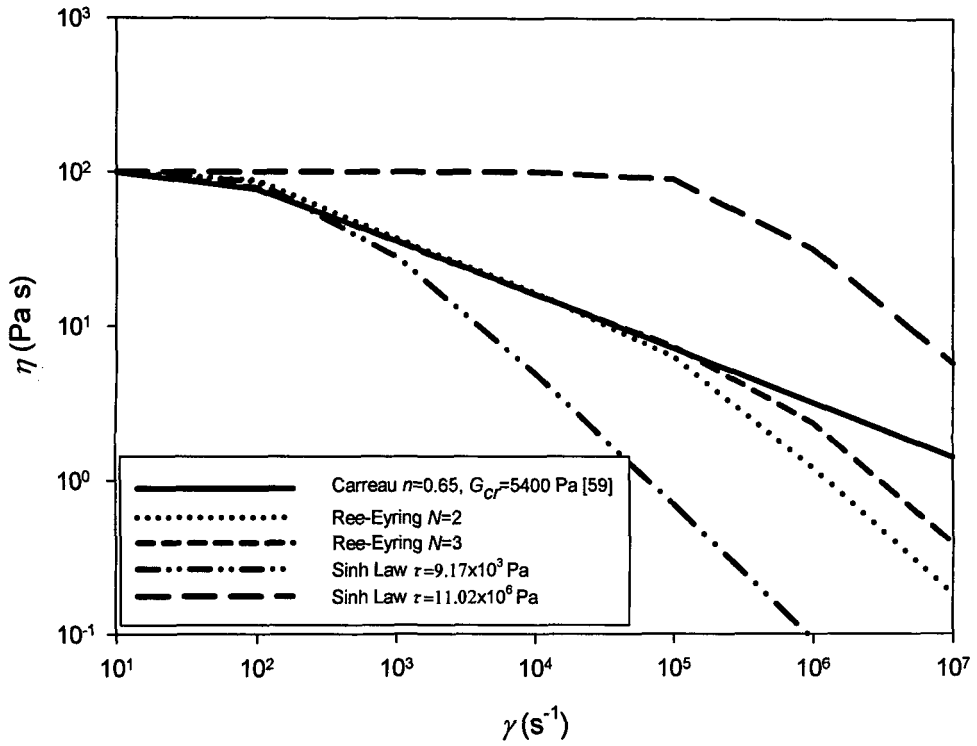

Fig.5.1 Comparison of Carreau, Ree Eyring (2 and 3 flow units) and sinh law models for LF 5346 gear oil

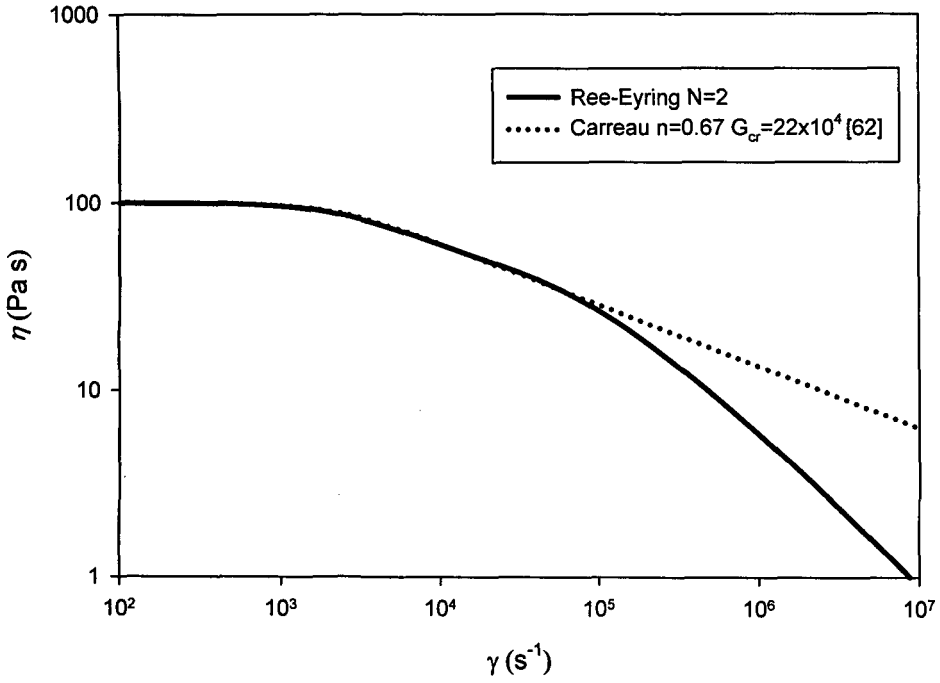

Fig.5.2 Comparison of Carreau and Ree Eyring (2 flow units) models for PG 460 oil

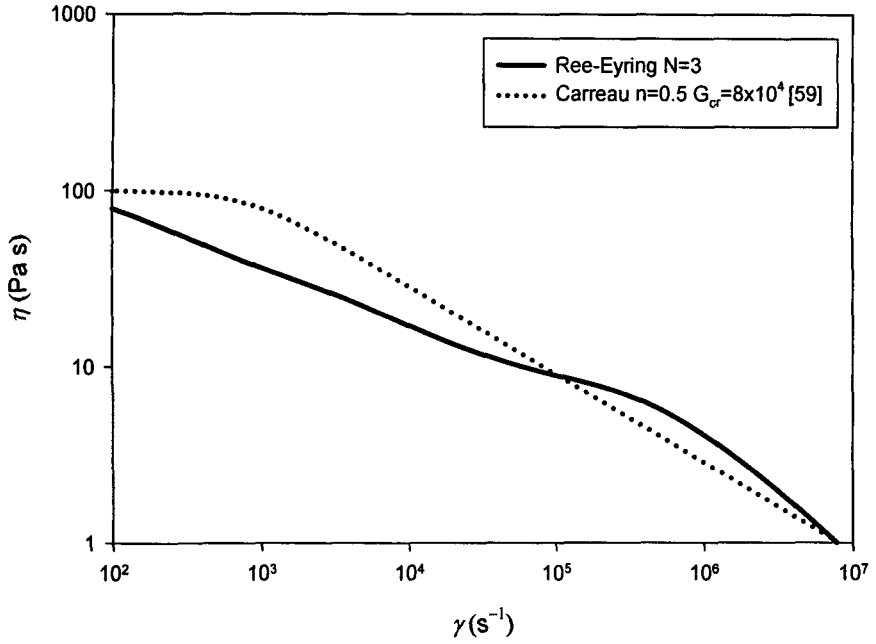

Fig.5.3 Comparison of Carreau and Ree-Eyring (3 flow units) models for PDMS oil

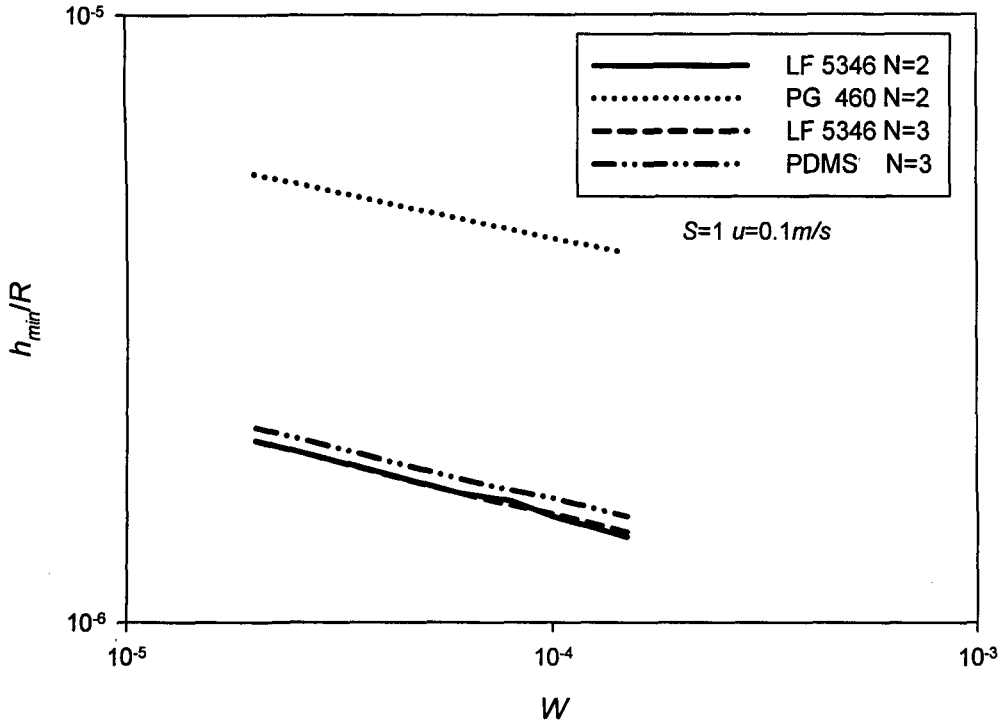

Fig.5.4 Variation of dimensionless minimum film thickness for LF 5346 gear oil (2 and 3 flow units), PG 460 and PDMS oil (2 flow units) at u=0.1m/s and S=1

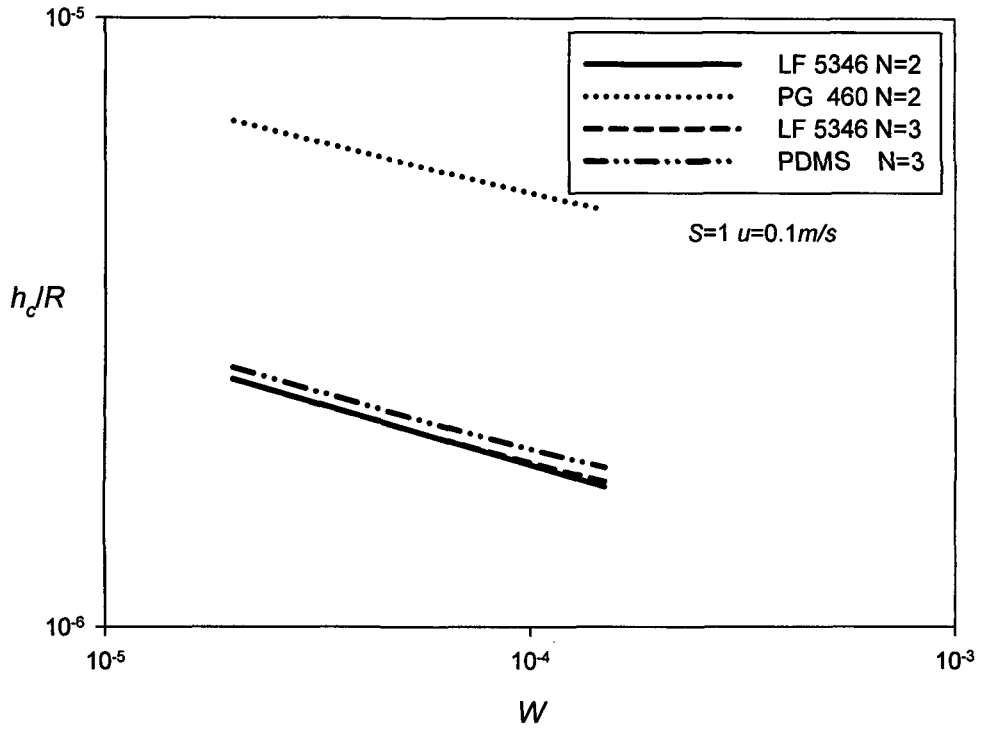

Fig.5.5 Variation of dimensionless central film thickness for LF 5346 gear oil (2 and 3 flow units), PG 460 and PDMS oil (2 flow units) at u=0.1m/s and S=1

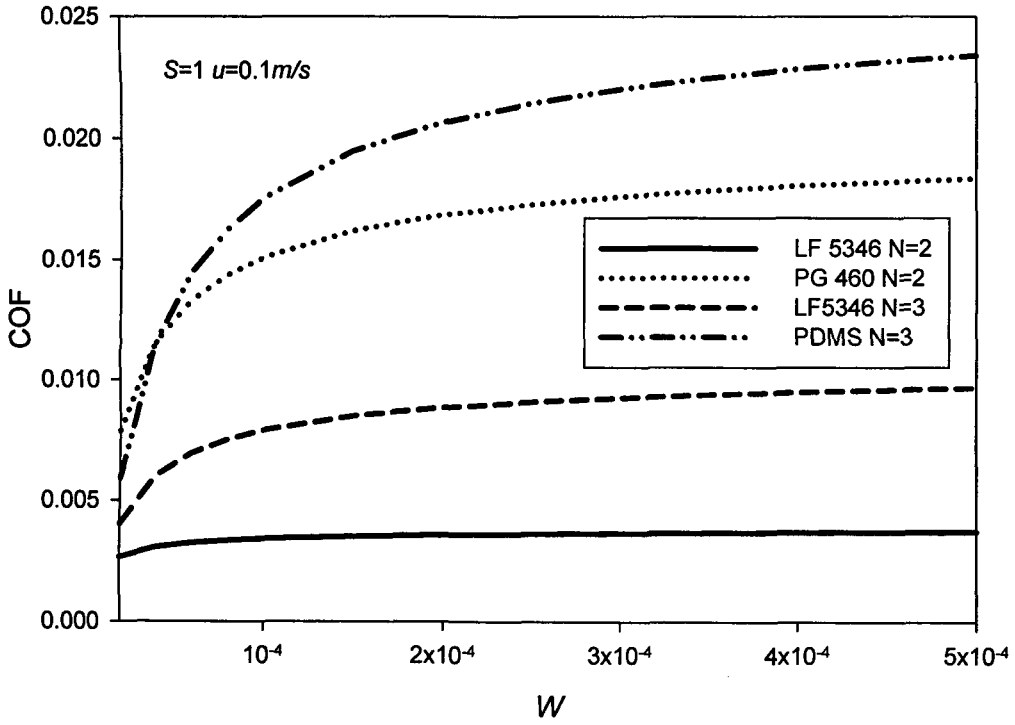

Fig.5.6 Variation of coefficient of friction for LF 5346 gear oil (2 and 3 flow units), PG 460 and PDMS oil (2 flow units) at u=0.1m/s and S=1

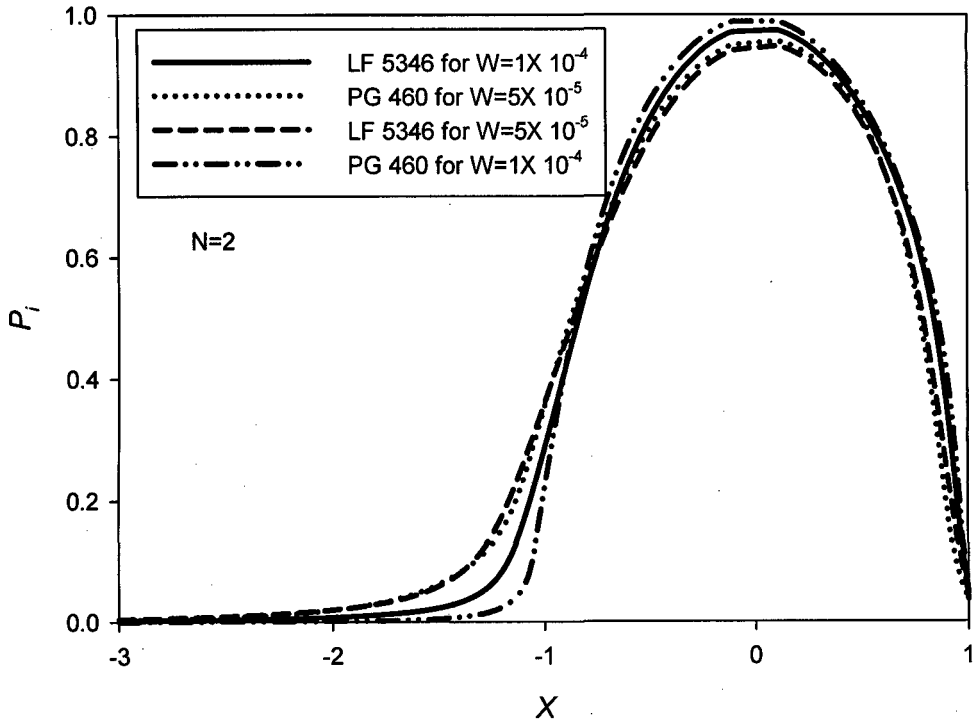

Fig.5.7 Variation of pressure distribution for LF 5346 Gear oil and PG 460 oil (2 flow units) at u=0.1m/s and S=1

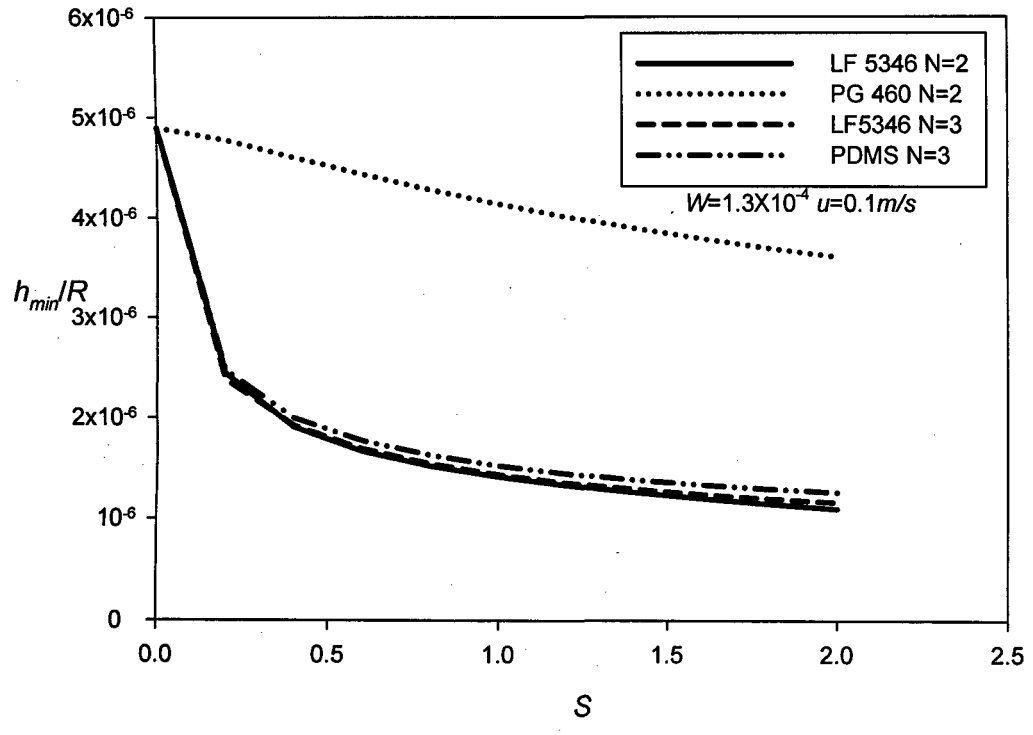

Fig.5.8 Variation of dimensionless minimum film thickness for LF 5346 gear oil (2 and 3 flow units), PG 460(2 flow units) and PDMS (3 flow units) oil at W=1.3X10^{-4} and u=0.1 m/s

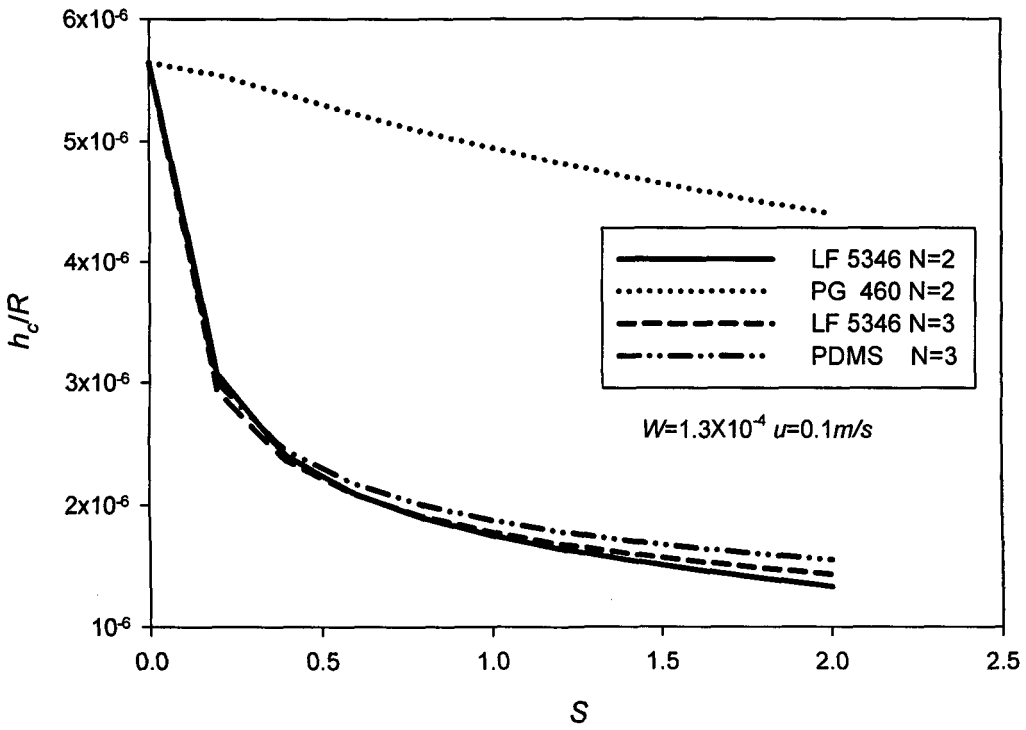

Fig.5.9 Variation of dimensionless central film thickness for LF 5346 gear oil (2 and 3 flow units), PG 460(2 flow units) and PDMS (3 flow units) oil at W=1.3X10^{-4} and u=0.1 m/s

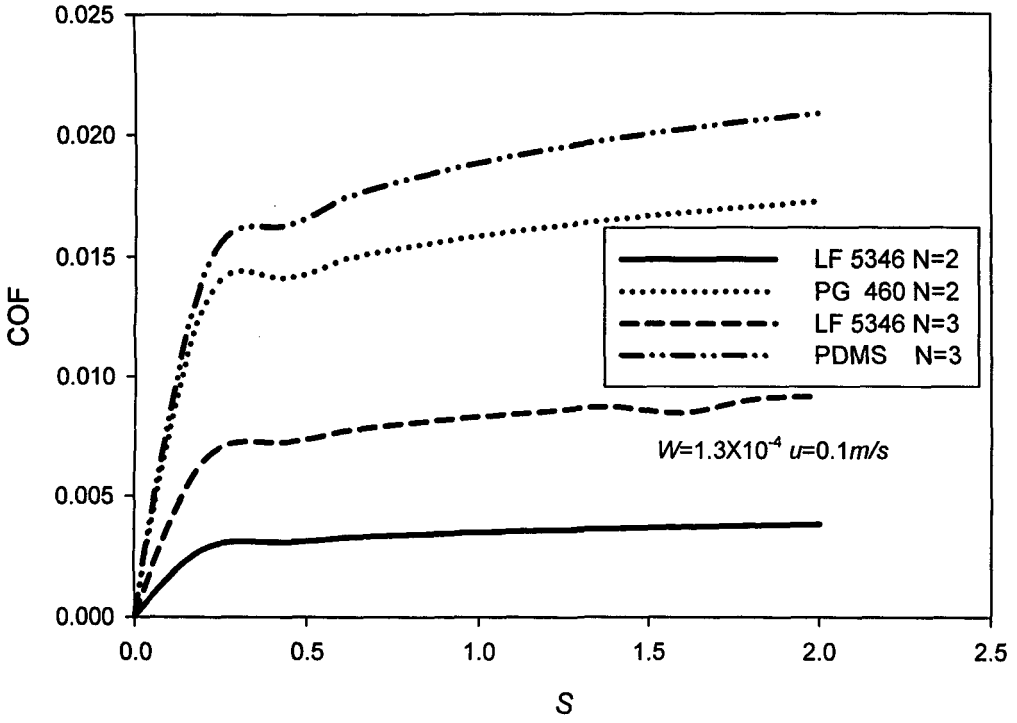

Fig.5.10 Variation of coefficient of friction for LF 5346 gear oil (2 and 3 flow units), PG 460(2 flow units) and PDMS (3 flow units) oil at *W*=1.3X10^{-4} and *u*=0.1 *m/s*

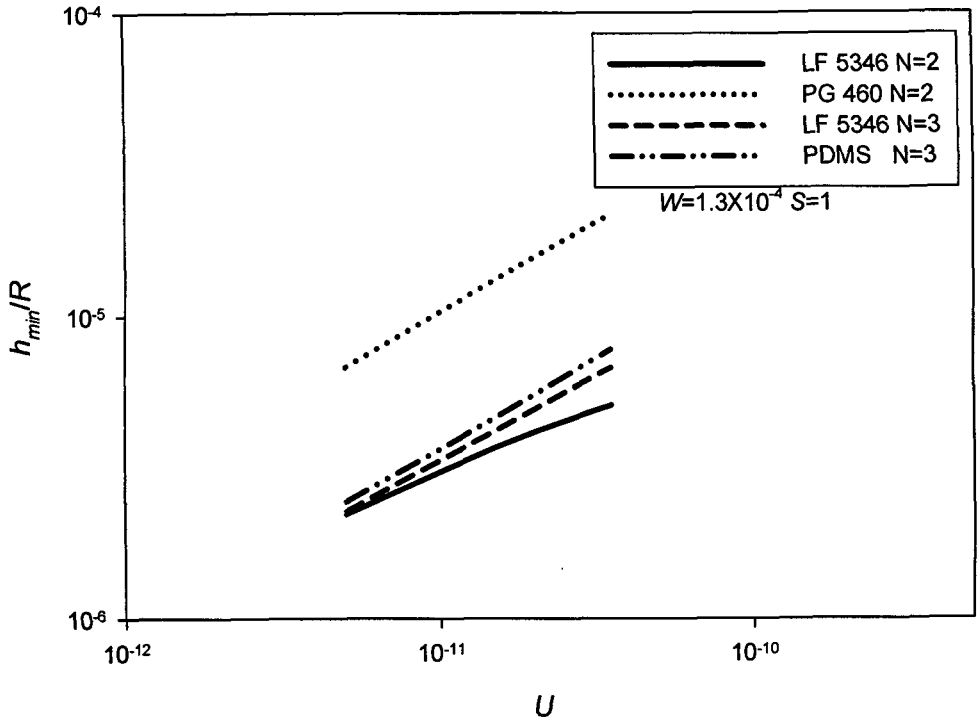

Fig.5.11 Comparison of dimensionless minimum film thickness for LF 5346 oil (2 and 3 flow units), PG 460(2 flow units) and PDMS(3 flow units) oil at W=1.3X10^{-4} and S=1

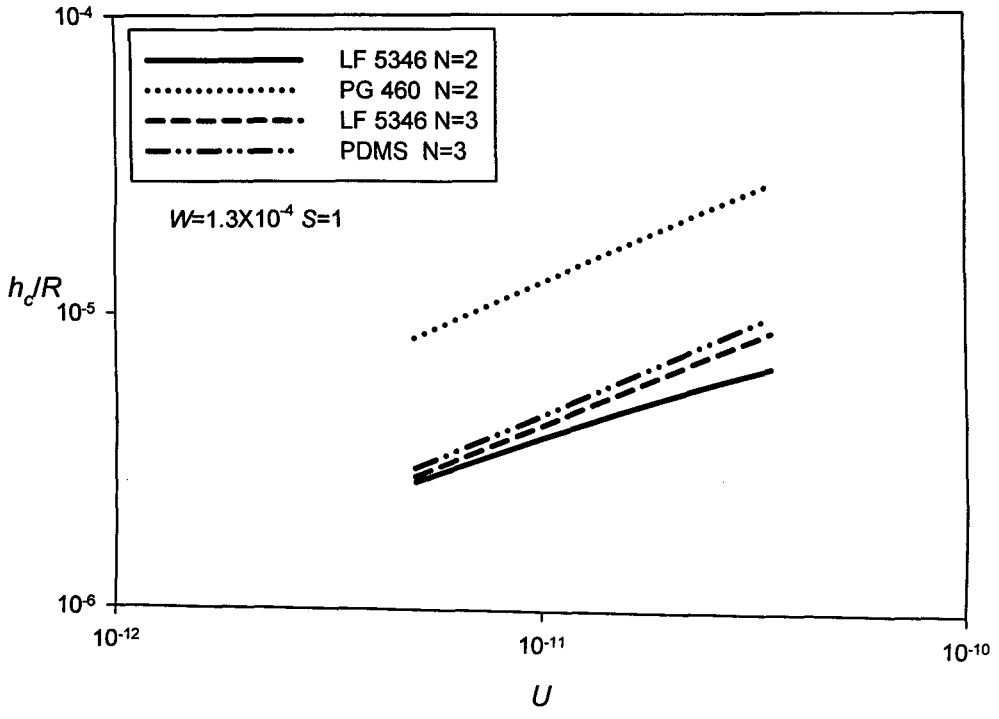

Fig.5.12 Variation of dimensionless central film thickness for LF 5346 gear oil (2 and 3 flow units), PG 460(2 flow units) and PDMS (3 flow units) oil at W=1.3X10^{-4} and S

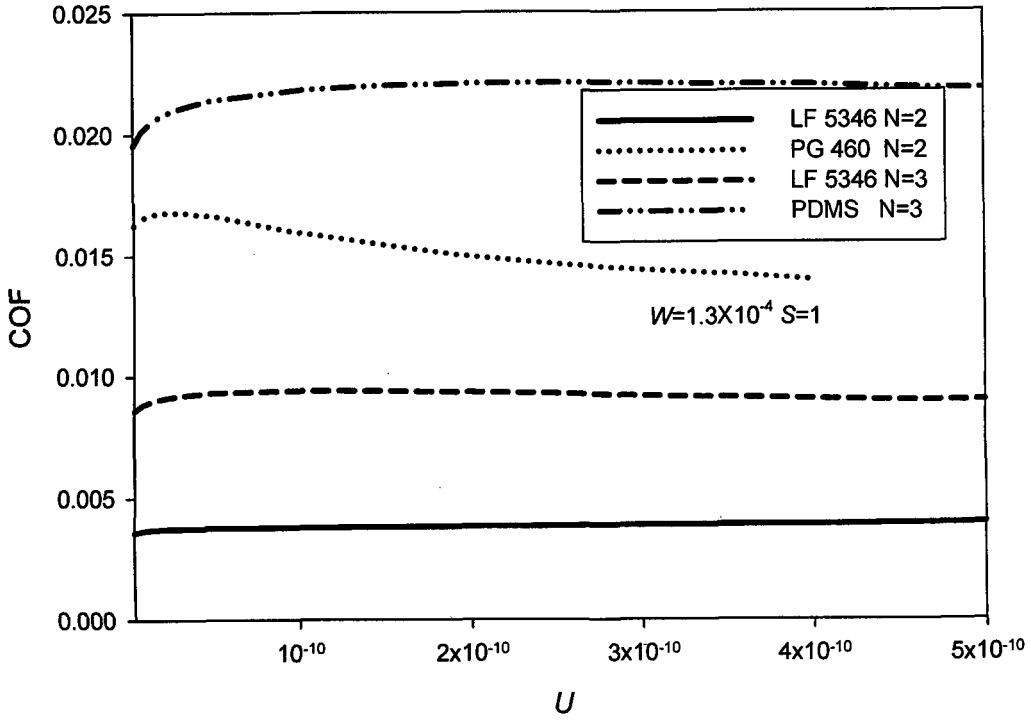

Fig.5.13 Variation of coefficient of friction for LF 5346 gear oil (2 and 3 flow units), PG 460(2 flow units) and PDMS (3 flow units) oil at W=1.3X10^{-4} and S=1

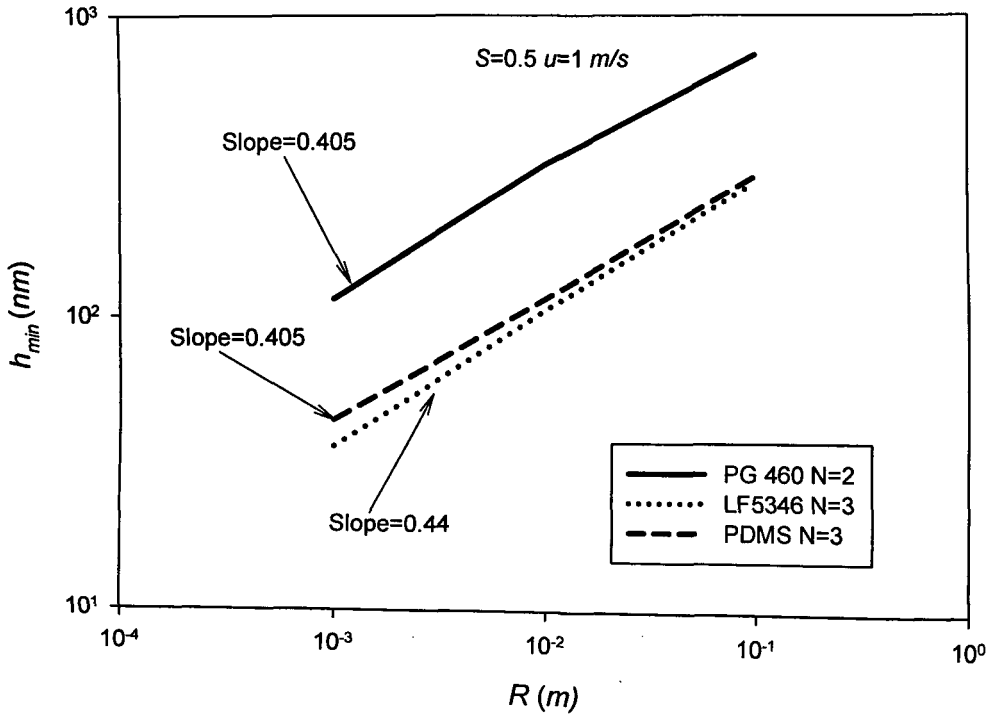

Fig.5.14 Variation of minimum film thickness with radius for LF 5346 gear oil (2 and 3 flow units), PG 460(2 flow units) and PDMS (3 flow units) oil at u=1m/s and S=0.5

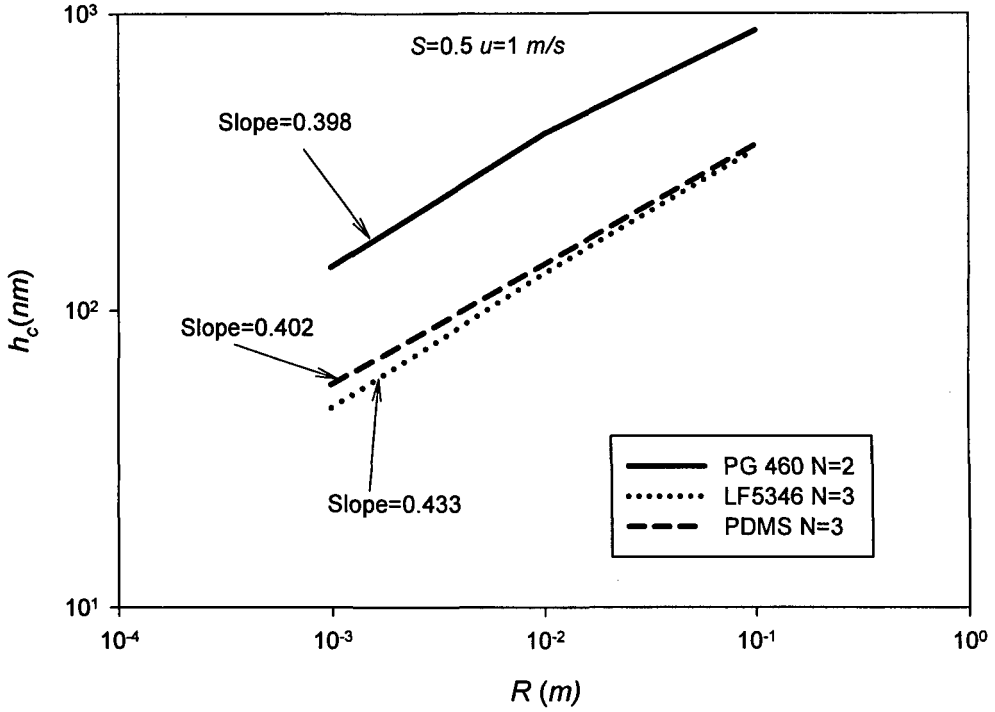

Fig.5.15 Variation of central film thickness with radius for for LF 5346 gear oil (2 and 3 flow units), PG 460(2 flow units) and PDMS (3 flow units) oil at u=1m/s and S=0.5

Chapter 6

CONCLUSIONS AND SCOPE FOR FUTURE WORK

6.1 Concluding remarks

The present study numerically investigates the effect of shear thinning behaviour using actual Ree-Eyring model with different number of flow units for three different types of oils. The results are obtained to study the effect of load, speed, slide to roll ratio and radius of curvature on the EHL characteristics. On the basis of the results presented in Chapter 5, the following conclusions are drawn:

1. The popular form of Ree-Eyring model with only one flow unit fails to describe realistic flow behaviour of EHL lubricants while the actual Ree-Eyring model with multiple flow units exhibits good agreement with Carreau model.

2. The departure of Ree-Eyring model from Carreau model can be minimized by increasing the number of flow units.

3. The lubricant rehology observed from the $\eta - \dot{\gamma}$ curves indicates that LF 5346 gear oil is the most shear-thinning lubricant of the three oils, whereas, PG 460 oil exhibits a much less pronounced shear-thinning behaviour.

4. The EHL film thickness sensitivity to maximum Hertzian pressure (p_H) increase with increasing shear-thinning behaviour of three oils – this effect is very well captured by the Ree-Eyring model.

5. The COF increases with increasing value of the load parameter W, however, with a decreasing rate due to increasing shear-thinning effect at higher loads. Also, it may be concluded that using lesser number of flow units underestimates the value of coefficient of friction.

6. The consideration of 2 flow units in the Ree-Eyring model is sufficient from the viewpoint of film thickness prediction. However, for highly shear-thinning oils at high speeds, at least 3 flow units are required to model the lubricant rheology accurately.

7. The sensitivity of EHL film thickness to speed parameter decreases with increasing shear-thinning effect (i.e., in the order PG 460, PDMS and LF 5346). Hence, the use of classical film thickness formulas developed for Newtonian fluids may lead to large errors in the estimation of film thickness.

8. Shear-thinning effect has been found to be more pronounced at smaller radius. This effect is successfully captured by the Ree-Eyring model.

6.2 Scope for future work

It is well known that lubricants exhibit limiting shear strength behavior at high shear rates. Therefore, it would be a good idea to include this phenomenon in the future investigations. Also, the present work can be extended to circular and elliptical contacts which are encountered in various tribological components.

Chapter 7

REFERENCES

1. Stachowiak, G. W. and Batchelor, A. W., "Engineering Tribology" Elsevier Science, 1993.
2. Bair, S., "High-Pressure Rheology for Quantitative Elastohydrodynamics" Elsevier Science, 2007.
3. Dowson, D. and Higginson, G. R., "Elasto-hydrodynamic Lubrication" Pergamon Press, 1966.
4. Martin, H.M., "Lubrication of Gear Teeth" Engineering, Lond., vol.102,199, 1916.
5. Peppler, W., "Untersuchungen tiber die Drucktibertragung bei belasteten und geschmierten umlaufenden achsparallelen Zylindem," Maschine nelemente Tagung Aacgan 1935, 42, V. D. I., Verlag, Berlin, 1936.
6. Meldahl, A., "Contribution to the theory of lubrication of gears and of the stressing of the lubricated flanks of gear teeth," Brown Boveri Review, vol. 28, No. 11,374, 1941.
7. Gatcombe, E. K., "Lubrication characteristics of in volute spur gears- a theoretical investigation," Trans., Amer. Soc. Mech. Engrs, vol. 67, 177, 1945.
8. Hersey, M. D., and Lowdenslager, D. B., "Film thickness between gear teeth," Trans., Amer. Soc. Mech. Engrs, vol. 72, 1035, 1950.
9. Dorr, J., "Schmiermitteldruck Randverformungen des Rollenlagers," Ingenieur Archiv, vol. 22, No.3, 171, 1954.
10. Grubin, A. N., and Vinooradova, L. E., "Central Scientific Research Institute for technology and Mechanical Engineering," Book no. 30, Moscow, (D. S. I. R, Translation No. 337), 1949.
11. Petrusevich, A. I., "Fundamental conclusions from the contact hydrodynamic theory oflubrication," Izo. Akad. Nouk. SSSR (OTN), vol. 2, 209, 1950.

12. Weber, C. and Saalfeld, K., "Schmierfilmbei Walzen mit verformung," Zeits. Ang. Math. Mech. vol. 34, (Nos. 1-2), 54, 1954.

13. Crook, A. W., "The lubrication of rollers, I," Phil. Trans., A250, 387, 1958.

14. Crook, A. W., "The lubrication of rollers, II, Film thickness with relation to viscosity and speed," Phil. Trans. A254, 223, 1961.

15. Crook, A. W., "The lubrication of rollers, IV, Measurements of friction and effective viscosity," Phil. Trans., A255, 281, 1963.

16. Sibley, L. B. and Orcutt, F. K., "Elasto-hydrodynamic lubrication of rolling contact surfaces," Trans. Amer. Soc. Lub. Engrs., vol. 4 (2), 234, 1961.

17. Dowson, D. and Higginson, G. R., "A numerical solution to the elasto hydrodynamic problem," J. Mech. Engng. Sci., vol. 1, No.1, 6, 1959.

18. Dowson, D. and Higginson, G. R., "The theory of roller bearing lubrication and deformation," Inst. Mech. Engrs, Lubrication and Wear Convention, 1963.

19. Dowson, D. and Higginson, G. R., "New roller-bearing lubrication formula," Engineering Lond., vol. 192, 158, 1961.

20. Dowson, D., Higginson, G. R. and Whitaker, A. V., "Elasto-hydrodynamic lubrication - a survey of isothermal solutions," J. Mech. Engng. Sci., vol. 4, 2, 121, 1962.

21. Lewicki, W., "Hydrodynamic lubrication of roller bearings," Engineer, Lond, vol. 197, 920, 1954.

22. Dawson, P. H., "The pitting of lubricated gear teeth and rollers," Power Transmission, vol. 30, No. 351,208, 1961.

23. Bell, I. F., "Elasto-hydrodynamic effects in lubrication," M.Sc. Thesis, University of Manchester, 1961.

24. Milne, A. A., "A theory ofrheodynamic lubrication for a Maxwell liquid," Instn. Mech. Engrs., Proc. of the Conference on Lubrication and Wear, Paper 41, 66, 1957.

25. Tanner, R. I., "Full-film lubrication theory for a Maxwell liquid," Int. J. Mech. Sci., vol. 1,206, 1960.

26. Burton, R. A., "An analytical investigation of viscoelastic effects in the lubrication of rolling contact," Tranc. Amer. Soc. Lub. Engrs., vol. 3, No.1, 1, 1960.

27. Misharin, J. A., "Influence of the friction conditions on the magnitude of the friction coefficient in the case of rolling with sliding," Instn. Mech. Engrs., Proc. of the International Conference on Gearing, Paper 40, 159, 1958.

28. Sternlicht, B., Lewis, P. and Flynn, P., "Theory of lubrication and failure of rolling contacts," Trans. Amer. Soc. Mech. Engrs., J. of Basic Engineering, vol. 83, Series D, 2, 213, 1961.

29. Archard, G. D., Gair, F. C. and Hirst, W., "The elasto-hydrodynamic lubrication of rollers," Proc. Roy. Soc. A262, 51, 1961.

30. Osterle, J. F. and Stephenson, R. R., "A direct solution of the elasto hydrodynamic lubrication problem," Trans. Amer. Soc. Lub. Engrs., vol. 5, No. 2,365, 1962.

31. Ree, T. and Eyring, H., "Theory of Non-Newtonian Flow, I., Solid Plastic Systems; II., Solution Systems of High Polymers," J. Appl. Phys., vol. 26, No.7, pp. 795-809, 1954.

32. Hirst, W. and Moore, A. J., "Non-Newtonian Behaviour in Elastohydrodynamic Lubrication," Proc. Roy. Soc. London, Series A, vol. 337, p. 101, 1974.

33. Johnson, K. L. and Tevaarwerk, J. L., "Shear behaviour ofEHD Oil Films," Proc. Roy. SO,c. London, Series A, vol. 356, pp. 215-236, 1977.

34. Berthe, D., Houpert, L. and Flamand, L., "Thermal Effects in EHD Contacts for Different Rheological Behaviours of the Lubricant," Proc. of the 6th Leeds-Lyon Symposium, England, 1979.

35. Johnson, K. L. and Greenwood, J. A., "Thennal Analysis of an Eyring Fluid in EHD Traction," Wear, vol. 61, p. 353, 1980.

36. Houpert, L. G. and Hamrock, B. J., "Elastohydrodynamic Lubrication Calculations Used as a Tool to Study Scuffling," Proc. of the 12th Leeds-Lyon Symposium, London, pp. 146-159, 1985.

37. Conry, T. F., Wang, S. and Cusano, C., "A Reynolds-Eyring Equation for Elastohydrodynamic Lubrication in Line Contacts," ASME Journal of Tribology, vol. 107, pp. 648-658, 1987.

38. Chang, L., Cusano, C. and Conry, T. F., "Effects of Lubricant Rheology and Kinematic Conditions Micro-Elastohydrodynamic Lubrication," ASME Journal of Tribology, vol. 111, pp. 344, 1988.

39. Bair, S. and Winer, W.O., "A Rheological Model for Elastohydrodynamic Contacts Based in Primary Laboratory Data," ASME Journal of Lubrication Technology, vol. 101, No.3, pp. 258-265, 1979.

40. Gecim, B. and Winer, W.O., "Lubricant Limiting Shear Stress Effect on EHD Film Thickness," ASME Journal of Lubrication Technology, vol. 102, p. 213, 1980.

41. Jacobson, B. O. and Hanrock, B. J., "Non-Newtonian Fluid Model Incorporated into Elastohydrodynamic Lubrication of Rectangular Contacts," ASME Journal of Tribology, vol. 106, pp. 275-284, 1984.

42. Livonen, H. T. and Hamrock, B. J., "A Non-Newtonian Fluid Model for Elastohydrodynamic Lubrication of Rectangular Contacts," Proc. 5th International Congress on Tribology, 1989.

43. Lee, R. T. and Hanrock, B. J., "A Circular Non-Newtonian Fluid Model: Part 1 Used in Elastohydrodynamic Lubrication," ASME Journal of Tribology, vol. 112, pp. 486-496, 1990.

44. BhattachaJ:jee, R. C. and Das, N. C., "Power Law Fluid Model Incorporated into Elastohydrodynamic Lubrication Theory of Line Contact," Tribology International, vol. 29, pp. 405-413, 1996.

45. Tayal, S. P., Sinhasan, R. and Singh, D. V., "Analysis of Hydrodynamic Journal Bearing with Non-Newtonian Power law Lubricants by the Finite Element Method," Wear, vol. 71, pp. 15-27, 1981.

46. Evans, C. R. and Johnson, K. L., "The Rheological Properties of Elastohydrodynamic Lubrication," Proc. Instt. Mech. Engr., vol. 200, No. C5, pp. 301-312, 1986.

47. Kim, K. H. and Sadeghi, F., "Non-Newtonian Elastohydrodynamic Lubrication of Point Contact," ASME Journal of Tribology, vol. 113, pp. 703-711, 1991.

48. Sharif, K. J. H., Holt, C. A., Evans, H. P. and Snidle, R. W., "Simplfied Analysis of Non-Newtonian Effects in a Circular Elastohydrodynamic Contact and Comparison with Theory," STLE Tribology Transactions, vol. 42, pp. 39-45, 1999.

49. Stahl Jonas, and Jacobson, Bo. O., "A Non-Newtonian Model Based on Limiting Shear Stress and Slip Planes - Parameric Studies," Tribology International, vol. 36,pp.801-806,2003.

50. Wolff, R. and Kubo, A., "A Generalized Non-Newtonian Fluid Model Introduced into Elastohydrodynamic Lubrication," ASME Journal of Tribology, vol. 118, pp. 74-82, 1996.

51. http://www.tribology-abc.com/default.htm

52. Kumar, P., Jain , S. C., and Ray, S, Thermal EHL of rough rolling/ sliding line contacts using a mixture of two fluids at dynamic load, ASME, J. Tribol., 2002, 124, 709-715.

53. Damiens, B., Venner, C.H., Cann, P. M. E., and Lubrecht, A.A., 2004, "Starved Lubrication of Elliptical EHD Contacts," ASME J. Tribol., 126, pp. 105-111.

54. Chevalier, F., Lubrecht, A.A., Cann, P.M.E., Colin, F., and Dalmaz , G., 1998, "Film Thickness in Starved EHL Point Contacts," ASME J. Tribol., 120,pp. 126-133.

55. Houpert, L. G. and Hamrock, B. J., "Fast Approach for Calculating Film Thickness and Pressures in Elastohydrodynamically Lubricated Contacts at High Loads," ASME Journal of Tribology, vol. 108, pp. 411-419, 1986.

56. Venner, C. H., Napel, W. E. ten and Bosma, R., "Advanced Multilevel Solution of the EHL Line Contact Problem," ASME Journal of Tribology, vol. 112, pp. 426-432, 1990.

57. Roelands, C. J. A., Vluger, J. C. and Waterman, H. I., "The Viscosity Temperature-Pressure Relationship for Lubricating Oils and its Correlation with the Chemical Construction," ASME Journal of Basic Engineering, pp. 601-610, 1963.

58. Sadeghi, F., and Sui, P. C., "Compressible Elastohydrodynamic Lubrication of Rough Surfaces," ASME Journal of Tribology, vol. 111, pp. 56-62, 1989.

59. Kumar,P., and Khonsari,M.M, "Full EHL Simulations Using Actual Ree-Erying Model for Shear Thinning Lubricants"ASME Journal of Tribology ,Vol.131, pp011802(1 -6) 2009.

60. Kumar,P., and Khonsari,M.M, "Combined Effects of Shear Thinning and Viscous Heating on EHL Characteristics of Rolling /sliding Line Contacts "ASME Journal of Tribology ,Vol.130, pp041505(1 -13) 2008.

61. Dien, I. K., and Elrod, H. G., 1983, "A Generalized Steady-State Reynolds Equation for Non-Newtonian Fluids, with Application to Journal Bearings" ASME J. Lub. Tech., **105**, pp. 385-390.

62. Bair, S., 2004, "Actual Eyring Models for Thixotropy and Shear-Thinning Experimental Validation and Application to EHD," ASME J. Tribol., **126**, pp. 728-732

Appendix -1

DERIVATIVES FOR JACOBIAN MATRIX IN NEWTON-RAPHSON FORMULATION

The derivatives of the residues, f_i, of the finite difference Reynolds equation (3.33) constituting the Jacobian matrix $[J]$,are calculated as follows: $\frac{\partial f_i}{\partial H_0} = \frac{1}{2}\left(\frac{\partial \varepsilon_{i+1}}{\partial H_0} + \frac{\partial \varepsilon_i}{\partial H_0}\right)\frac{P_{i+1} - P_i}{\Delta X^2} - \frac{1}{2}\left(\frac{\partial \varepsilon_{i-1}}{\partial H_0} + \frac{\partial \varepsilon_i}{\partial H_0}\right)\frac{P_i - P_{i-1}}{\Delta X^2} - K\frac{(\overline{\rho}_i - \overline{\rho}_{i-1})}{\Delta X}$

where,

$$\frac{\partial \varepsilon_i}{\partial H_0} = \frac{\overline{\rho}_i}{\overline{\eta}_i}\left(3H_i^2\right)$$

$$\frac{\partial f_i}{\partial P_j} = \frac{1}{2}\left(\frac{\partial \varepsilon_{i+1}}{\partial P_j} + \frac{\partial \varepsilon_i}{\partial P_j}\right)\frac{P_{i+1} - P_i}{\Delta X^2} + \varepsilon_{i+1/2}\frac{\left(k_{i+1,j} - k_{i,j}\right)}{\Delta X^2} - \frac{1}{2}\left(\frac{\partial \varepsilon_{i-1}}{\partial P_j} + \frac{\partial \varepsilon_i}{\partial P_j}\right)\frac{P_i - P_{i-1}}{\Delta X^2}$$
$$+ \varepsilon_{i-1/2}\frac{\left(k_{i-1,j} - k_{i,j}\right)}{\Delta X^2} - K\frac{\left(\overline{\rho}_i \partial H_i / \partial P_j + H_i \partial \overline{\rho}_i / \partial P_j - \overline{\rho}_{i-1}\partial H_{i-1} / \partial P_j - H_{i-1}\partial \overline{\rho}_{i-1} / \partial P_j\right)}{\Delta X}$$

$$k_{i-1,j} = \begin{cases} 0 & i-1 \neq j \\ 1 & i-1 = j \end{cases}, \quad k_{i,j} = \begin{cases} 0 & i \neq j \\ 1 & i = j \end{cases}, \quad k_{i+1,j} = \begin{cases} 0 & i+1 \neq j \\ 1 & i+1 = j \end{cases}$$

$$\frac{\partial \varepsilon_i}{\partial P_j} = \frac{\overline{\rho}_i}{\overline{\eta}_i}\left(3H_i^2 \partial H_i / \partial P_j\right) + H_i^3\left(\frac{\overline{\eta}_i \partial \overline{\rho}_i / \partial P_j - \overline{\rho}_i \partial \overline{\eta}_i / \partial P_j}{\overline{\eta}_i^2}\right)$$

$$\frac{\partial \overline{\eta}_i}{\partial P_j} = 5.1\times10^{-9} k_{ij} p_h \overline{\eta}_i z\left(\ln \eta_o + 9.67\right)\left(1 + 5.1\times10^{-9} P p_h\right)^{z-1}$$

$$\frac{\partial \overline{\rho}_i}{\partial P_j} = \frac{0.6\times10^{-9} k_{ij} p_h}{\left(1 + 1.7\times10^{-9} P_i p_h\right)^2}\left(1 - \beta\left(\overline{\theta}_{m,i} - 1\right)\theta_o\right)$$